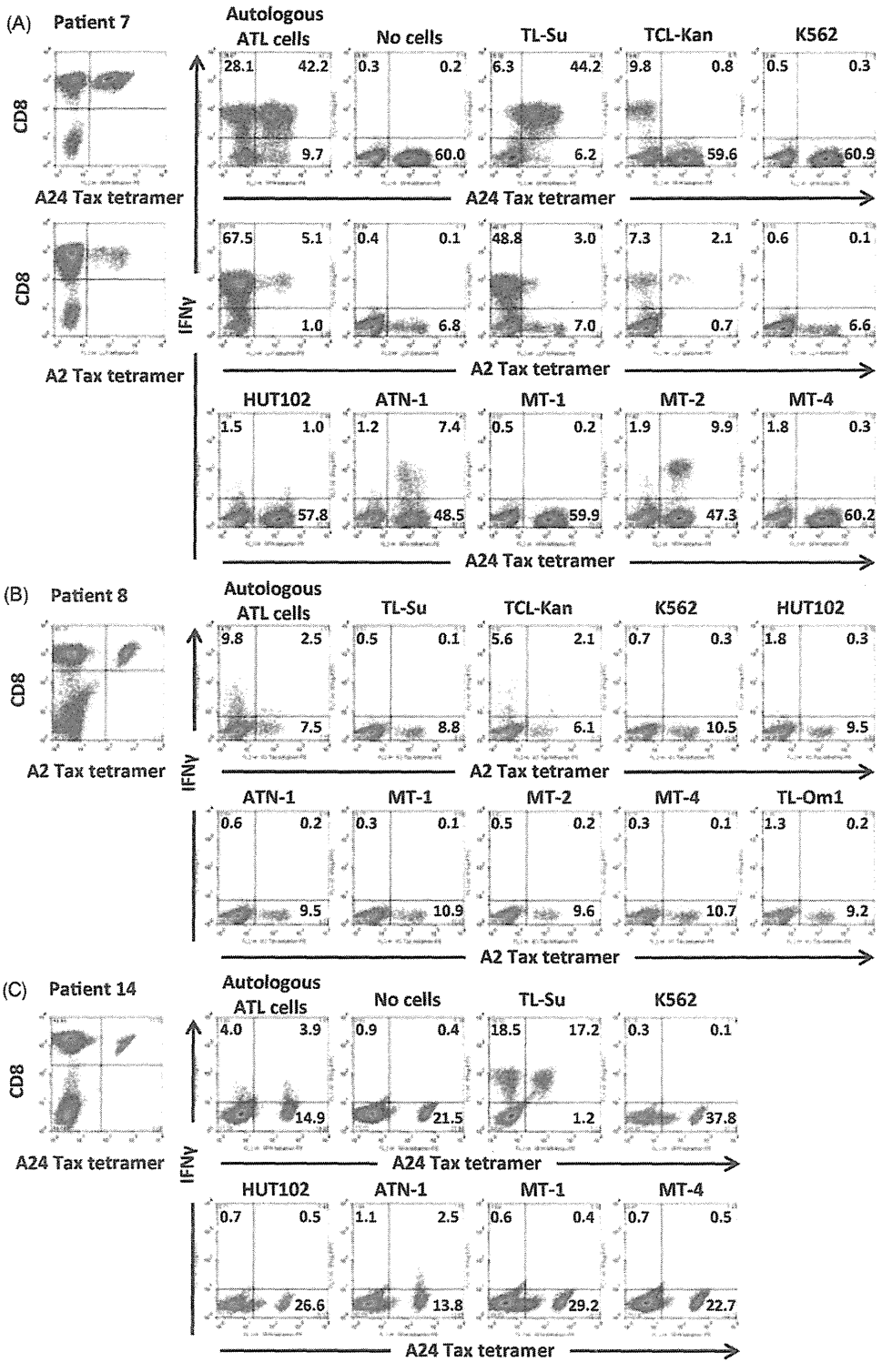

Fig. 4. Tax-specific CTL responses against autologous adult T-cell leukemia/lymphoma (ATL) cells. (A) PBMC from patient 7 were stimulated with human leukocyte antigen (HLA)-A*24:02 restricted Tax301–309 peptide, and the resulting CTL were expanded (upper-left panel). In this culture, HLA-A2-restricted Tax11–19 specific CTL were also expanded (middle-left panel). The expanded cells were co-cultured with autologous ATL cells, ATL cell lines, human T-lymphotropic virus type 1 (HTLV-1)-immortalized lines and K562 (all CD8-negative) for 4 h. CD8-positive cells are plotted according to HLA-A*24:02/Tax301–309 or HLA-A*02:01/zax11–19 tetramer-positivity and interferon gamma (IFN-γ) production, and the percentages in each quadrant are presented in the panels. (B) PBMC from ATL patient 8 at chronic stage were stimulated by Tax11–19 peptide, and the expanded cells co-cultured with the same range of cells as in (A). CD8-positive cells are plotted by HLA-A*0201/Tax11–19 tetramer positivity and IFN-γ production. The HLA-A*02:01/Tax11–19 tetramer recognized HLA-A*02:07-restricted Tax11–19 specific CTL. (C) PBMC from ATL patient 14 were stimulated with Tax301–309 peptide, and treated as in (A, B) above. Each result represents three independent experiments.

doi: 10.1111/j.1349-7006.2012.02371.x

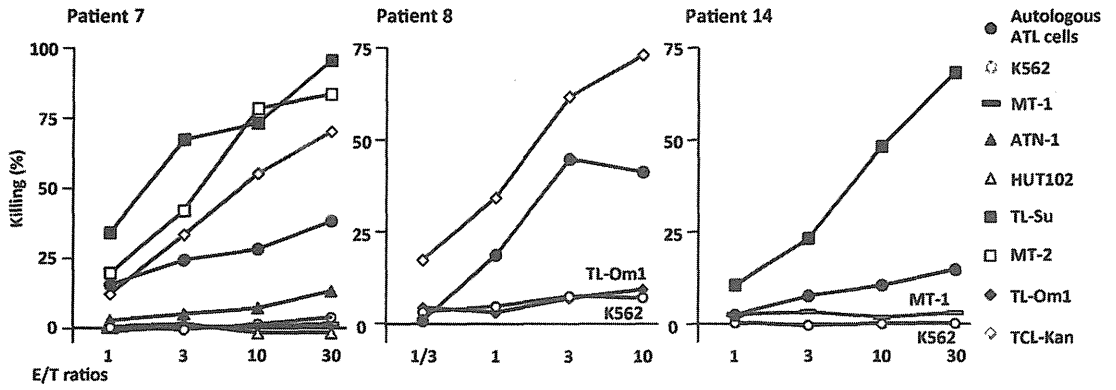

Fig. 5. Lysis of autologous adult T-cell leukemia/lymphoma (ATL) cells by Tax-specific CTL. Tax301–309 peptide-expanded cells from ATL patient 7 (left panel), Tax11–19 peptide-expanded cells from patient 8 (middle panel) and Tax301–309-stimulated patient 14 (right panel) were evaluated for cytotoxicity by a standard 4-h chromium[51] release assay. Lysis was restricted to human leukocyte antigen (HLA)-A*24:02 or HLA-A2 and Tax-positive target cells. Each result represents three independent experiments.

AC. However, in these reports, the nature of the antigens recognized by the CTL is not determined, or the target cells are HTLV-1-infected T-cell lines rather than primary ATL tumor cells. In contrast, the present study clearly demonstrated that Tax antigen expressed by ATL cells was a significant target for CTL from ATL patients in an autologous setting. In addition, Tax expression was observed only in actively cycling ATL cells. This could only be noticed in primary ATL cells from patients, because established ATL cell lines or HTLV-1-immortalized lines, which are commonly used for many types of experiments, are, of course, continuously dividing. These findings collectively demonstrate that the main obstacle to successful immunotherapy targeting Tax, with its very limited expression in ATL cells, could be overcome. Whether primary ATL cells express Tax has been examined in several other studies using tumor cells from patients' blood.[11,12,33] However, the present study demonstrated that most primary ATL cells in the blood are in a quiescent state, in which they express little or no Tax. Proliferating ATL cells are probably mostly to be found in lymph nodes in humans, not in the blood,[35] and these should, therefore, express substantial levels of Tax. Thus, the present findings indicate that Tax is a promising molecular target for immunotherapy in ATL patients, such as adoptive T-cell therapy and/or active vaccination.

As mentioned above, the efficiency of *in vitro* Tax-CTL expansion depended on HTLV-1 disease status. There was a trend towards superior expansion of Tax-CTL in HTLV-1 AC, ATL patients with the indolent variant and ATL patients who were in treatment-induced remission compared with newly diagnosed ATL patients with the aggressive variant. These observations indicate that host immune responses against Tax

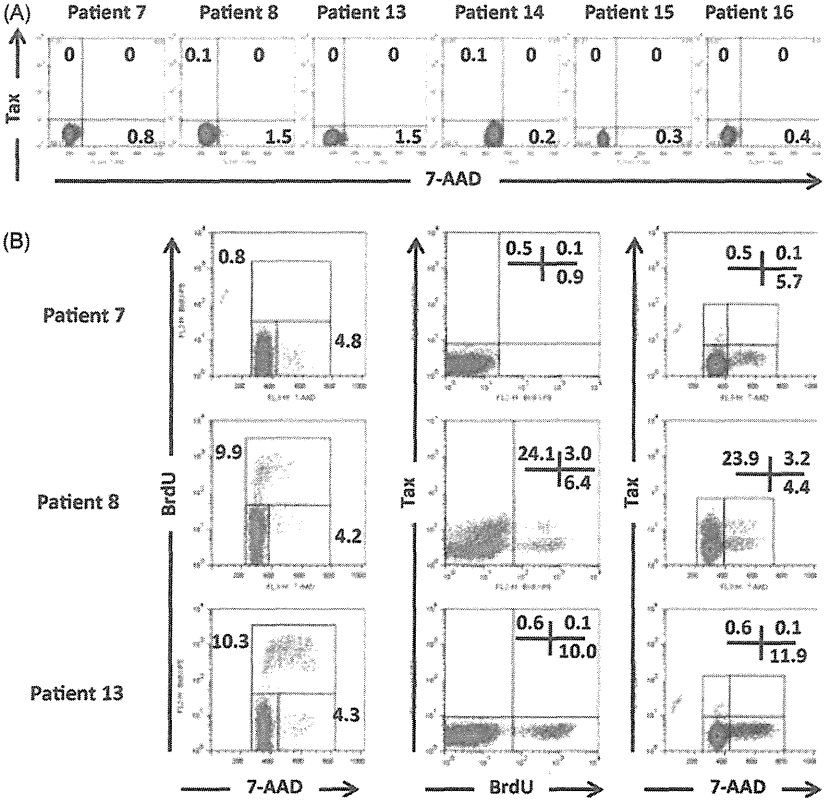

Fig. 6. Tax expression in adult T-cell leukemia/lymphoma (ATL) cells induced by short-term culture. (A) Lack of Tax expression in primary ATL cells from peripheral blood of patients 7, 8, 13, 14, 15 and 16. Cells were in a quiescent state as determined by 7-ADD staining. (B) Cell cycle status and Tax expression of short-term cultured primary ATL cells. Tax expression was induced when cells were actively cycling. Each result represents three independent experiments.

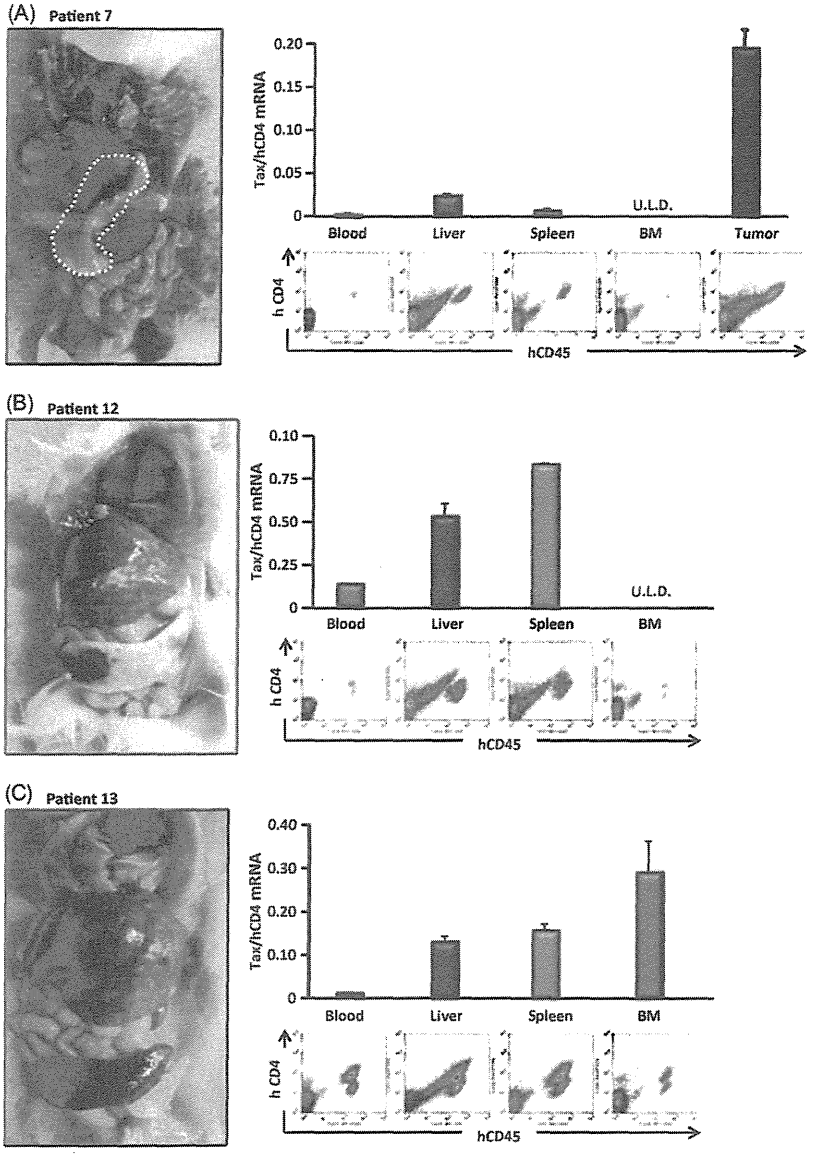

Fig. 7. Tax expression in primary adult T-cell leukemia/lymphoma (ATL) cell-bearing NOG mice. Tax expression of ATL cells in each affected organ of NOG mice bearing primary ATL cells from patient 7 (A), 12 (B) and 13 (C) were evaluated. NOG mice with cells from patient 7 presented with large intraperitoneal tumor masses demarcated by the white dotted lines. *Tax/human CD4* mRNA values of the cells from each organ are presented as bar graphs, where the value for TL-Su was set at unity. Flow cytometric analysis of the cells from each organ determined by human CD45 and CD4 expression is presented. Columns, mean of triplicate experiments; bars, standard deviation. BM, bone marrow; U.L.D., under limit of detection.

play an important role in maintaining the stable status of HTLV-1 AC, indolent ATL patients and ATL in remission. In addition, quantitative and/or functional reduction of Tax-CTL should lead to progression from HTLV-1 AC to ATL, or from indolent to aggressive ATL, or to relapse in ATL patients. Furthermore, the present observations suggest that restoration of substantial anti-Tax responses in some appropriate manner will lead to improvement of ATL disease status.

The efficient expansion of Tax-CTL from PBMC of ATL patients in remission suggests that reducing the number of tumor cells before Tax-targeted immunotherapy could be a crucial factor for successful induction/augmentation of antigen-specific CD8-positive CTL. We have reported that the humanized anti-CCR4 mAb KW-0761 (mogamulizumab) exerted clinically significant antitumor activity in relapsed ATL patients.[36,37] In addition, consistent with the fact that CCR4 is expressed not only on Th2 cells, but also on Treg cells,[21,38–40] KW-0761 treatment resulted in a significant and lasting decrease in CD4+CD25+FOXP3+ cells, including both the tumor cells and endogenous non-ATL Treg cells.[37] Reduction or suppression of Treg cells is expected to be a promising strategy for boosting antitumor immunity in cancer patients, as observed in studies with ipilimumab.[41,42] In fact, Tax-CTL were efficiently expanded from PBMC of patients 2 and 3 who were in CR after KW-0761 treatment. Thus, combining Tax-targeted immunotherapy following reduction of ATL cells and endogenous Treg cell depletion by KW-0761 treatment would be an ideal strategy for ATL immunotherapy.

The efficient expansion of Tax-CTL from PBMC of patients in remission after allogeneic HSCT is consistent with the report that Tax-specific CD8-positive T cells contribute to graft-versus-ATL effects.[13,43] Therefore, Tax-targeted immunotherapy after allogeneic HSCT should be therapeutically effective without increased graft-versus-host disease, which is a frequent and serious complication of this modality.

In conclusion, the present study not only provides a strong rationale for selecting Tax as a possible target for ATL immunotherapy but also contributes to our understanding of the immunopathogenesis driving progression from HTLV-1 AC to ATL, and to devising strategies for preventing this by targeting Tax.

doi: 10.1111/j.1349-7006.2012.02371.x

Acknowledgments

The present study was supported by Grants-in-Aid for Young Scientists (A) (No. 22689029, T. Ishida), Scientific Research (B) (No. 22300333, T Ishida and R. Ueda), and Scientific Support Programs for Cancer Research (No. 221S0001, T. Ishida) from the Ministry of Education, Culture, Sports, Science and Technology of Japan, Grants-in-Aid for National Cancer Center Research and Development Fund (No. 21-6-3, T. Ishida), and Health and Labour Sciences Research Grants (H22-Clinical Cancer Research-general-028, T. Ishida and H23-Third Term Comprehensive Control Research for Cancer-general-011, T. Ishida, H Nishikawa and H. Inagaki) from the Ministry of Health, Labour and Welfare, Japan.

Disclosure Statement

Nagoya City University Graduate School of Medical Sciences has received research grant support from Kyowa Hakko Kirin for works provided by Takashi Ishida. No other conflict of interest relevant to this article is reported.

References

1 Uchiyama T, Yodoi J, Sagawa K, Takatsuki K, Uchino H. Adult T-cell leukemia: clinical and hematologic features of 16 cases. *Blood* 1977; **50**: 481–92.
2 Matsuoka M, Jeang KT. Human T-cell leukaemia virus type 1 (HTLV-1) infectivity and cellular transformation. *Nat Rev Cancer* 2007; **7**: 270–80.
3 Hino S, Sugiyama H, Doi H *et al.* Breaking the cycle of HTLV-I transmission via carrier mothers' milk. *Lancet* 1987; **2**: 158–9.
4 Ishida T, Ueda R. Immunopathogenesis of lymphoma: focus on CCR4. *Cancer Sci* 2011; **102**: 44–50.
5 Shimoyama M. Diagnostic criteria and classification of clinical subtypes of adult T-cell leukaemia-lymphoma. A report from the Lymphoma Study Group (1984–87). *Br J Haematol* 1991; **79**: 428–37.
6 Akagi T, Ono H, Shimotohno K. Characterization of T cells immortalized by Tax1 of human T-cell leukemia virus type 1. *Blood* 1995; **86**: 4243–9.
7 Kannagi M, Sugamura K, Kinoshita K, Uchino H, Hinuma Y. Specific cytolysis of fresh tumor cells by an autologous killer T cell line derived from an adult T cell leukemia/lymphoma patient. *J Immunol* 1984; **133**: 1037–41.
8 Arnulf B, Thorel M, Poirot Y *et al.* Loss of the ex vivo but not the reinducible CD8+ T-cell response to Tax in human T-cell leukemia virus type I-infected patients with adult T-cell leukemia/lymphoma. *Leukemia* 2004; **18**: 126–32.
9 Kannagi M, Sugamura K, Sato H, Okochi K, Uchino H, Hinuma Y. Establishment of human cytotoxic T cell lines specific for human adult T cell leukemia virus-bearing cells. *J Immunol* 1983; **130**: 2942–6.
10 Kannagi M, Harada S, Maruyama I *et al.* Predominant recognition of human T cell leukemia virus type I (HTLV-I) pX gene products by human CD8+ cytotoxic T cells directed against HTLV-I-infected cells. *Int Immunol* 1991; **3**: 761–7.
11 Takeda S, Maeda M, Morikawa S *et al.* Genetic and epigenetic inactivation of tax gene in adult T-cell leukemia cells. *Int J Cancer* 2004; **109**: 559–67.
12 Kannagi M, Harashima N, Kurihara K *et al.* Tumor immunity against adult T-cell leukemia. *Cancer Sci* 2005; **96**: 249–55.
13 Harashima N, Kurihara K, Utsunomiya A *et al.* Graft-versus-Tax response in adult T-cell leukemia patients after hematopoietic stem cell transplantation. *Cancer Res* 2004; **64**: 391–9.
14 Ishida T, Utsunomiya A, Iida S *et al.* Clinical significance of CCR4 expression in adult T-cell leukemia/lymphoma: its close association with skin involvement and unfavorable outcome. *Clin Cancer Res* 2003; **9**: 3625–34.
15 Ri M, Iida S, Ishida T *et al.* Bortezomib-induced apoptosis in mature T-cell lymphoma cells partially depends on upregulation of Noxa and functional repression of Mcl-1. *Cancer Sci* 2009; **100**: 341–8.
16 Lozzio CB, Lozzio BB. Human chronic myelogenous leukemia cell line with positive Philadelphia chromosome. *Blood* 1975; **45**: 321–34.
17 Lee B, Tanaka Y, Tozawa H. Monoclonal antibody defining tax protein of human T-cell leukemia virus type-I. *Tohoku J Exp Med* 1989; **157**: 1–11.
18 Ishida T, Iida S, Akatsuka Y *et al.* The CC chemokine receptor 4 as a novel specific molecular target for immunotherapy in adult T-Cell leukemia/lymphoma. *Clin Cancer Res* 2004; **10**: 7529–39.
19 Mori F, Ishida T, Ito A *et al.* Potent antitumor effects of bevacizumab in a microenvironment-dependent human lymphoma mouse model. *Blood Cancer J* 2012; **2**: e67, doi:10.1038/bcj.2012.12 [Epub ahead of print].
20 Ishii T, Ishida T, Utsunomiya A *et al.* Defucosylated humanized anti-CCR4 monoclonal antibody KW-0761 as a novel immunotherapeutic agent for adult T-cell leukemia/lymphoma. *Clin Cancer Res* 2010; **16**: 1520–31.
21 Ishida T, Ueda R. CCR4 as a novel molecular target for immunotherapy of cancer. *Cancer Sci* 2006; **97**: 1139–46.
22 Kozako T, Arima N, Toji S *et al.* Reduced frequency, diversity, and function of human T cell leukemia virus type 1-specific CD8+ T cell in adult T cell leukemia patients. *J Immunol* 2006; **177**: 5718–26.
23 Kannagi M, Hasegawa A, Kinpara S *et al.* Double control systems for human T-cell leukemia virus type 1 by innate and acquired immunity. *Cancer Sci* 2011; **102**: 670–6.
24 Shimizu Y, Takamori A, Utsunomiya A *et al.* Impaired Tax-specific T-cell responses with insufficient control of HTLV-1 in a subgroup of individuals at asymptomatic and smoldering stages. *Cancer Sci* 2009; **100**: 481–9.
25 Kawano N, Shimoda K, Ishikawa F *et al.* Adult T-cell leukemia development from a human T-cell leukemia virus type I carrier after a living-donor liver transplantation. *Transplantation* 2006; **82**: 840–3.
26 Suzuki S, Uozumi K, Maeda M *et al.* Adult T-cell leukemia in a liver transplant recipient that did not progress after onset of graft rejection. *Int J Hematol* 2006; **83**: 429–32.
27 Yano H, Ishida T, Inagaki A *et al.* Regulatory T-cell function of adult T-cell leukemia/lymphoma cells. *Int J Cancer* 2007; **120**: 2052–7.
28 Choi EM, Chen JL, Wooldridge L *et al.* High avidity antigen-specific CTL identified by CD8-independent tetramer staining. *J Immunol* 2003; **171**: 5116–23.
29 Betts MR, Price DA, Brenchley JM *et al.* The functional profile of primary human antiviral CD8+ T cell effector activity is dictated by cognate peptide concentration. *J Immunol* 2004; **172**: 6407–17.
30 Itoh Y, Hemmer B, Martin R, Germain RN. Serial TCR engagement and down-modulation by peptide: MHC molecule ligands: relationship to the quality of individual TCR signaling events. *J Immunol* 1999; **162**: 2073–80.
31 Benlalam H, Linard B, Guilloux Y *et al.* Identification of five new HLA-B*3501-restricted epitopes derived from common melanoma-associated antigens, spontaneously recognized by tumor-infiltrating lymphocytes. *J Immunol* 2003; **171**: 6283–9.
32 Yoshikawa T, Nakatsugawa M, Suzuki S *et al.* HLA-A2-restricted glypican-3 peptide-specific CTL clones induced by peptide vaccine show high avidity and antigen-specific killing activity against tumor cells. *Cancer Sci* 2011; **102**: 918–25.
33 Kurihara K, Harashima N, Hanabuchi S *et al.* Potential immunogenicity of adult T cell leukemia cells in vivo. *Int J Cancer* 2005; **114**: 257–67.
34 Ito A, Ishida T, Utsunomiya A *et al.* Defucosylated anti-CCR4 monoclonal antibody exerts potent ADCC against primary ATLL cells mediated by autologous human immune cells in NOD/Shi-scid, IL-2R gamma(null) mice in vivo. *J Immunol* 2009; **183**: 4782–91.
35 Umino A, Nakagawa M, Utsunomiya A *et al.* Clonal evolution of adult T-cell leukemia/lymphoma takes place in the lymph nodes. *Blood* 2011; **117**: 5473–8.
36 Yamamoto K, Utsunomiya A, Tobinai K *et al.* Phase I study of KW-0761, a defucosylated humanized anti-CCR4 antibody, in relapsed patients with adult T-cell leukemia-lymphoma and peripheral T-cell lymphoma. *J Clin Oncol* 2010; **28**: 1591–8.
37 Ishida T, Joh T, Uike N *et al.* Defucosylated anti-CCR4 monoclonal antibody (KW-0761) for relapsed adult T-cell leukemia-lymphoma: a multicenter phase ii study. *J Clin Oncol* 2012; **30**: 837–42.
38 Imai T, Nagira M, Takagi S *et al.* Selective recruitment of CCR4-bearing Th2 cells toward antigen-presenting cells by the CC chemokines thymus and activation-regulated chemokine and macrophage-derived chemokine. *Int Immunol* 1999; **11**: 81–8.
39 Iellem A, Mariani M, Lang R *et al.* Unique chemotactic response profile and specific expression of chemokine receptors CCR4 and CCR8 by CD4(+) CD25(+) regulatory T cells. *J Exp Med* 2001; **194**: 847–53.
40 Ishida T, Ishii T, Inagaki A *et al.* Specific recruitment of CC chemokine receptor 4-positive regulatory T cells in Hodgkin lymphoma fosters immune privilege. *Cancer Res* 2006; **66**: 5716–22.
41 Hodi FS, O'Day SJ, McDermott DF *et al.* Improved survival with ipilimumab in patients with metastatic melanoma. *N Engl J Med* 2010; **363**: 711–23.
42 Robert C, Thomas L, Bondarenko I *et al.* Ipilimumab plus dacarbazine for previously untreated metastatic melanoma. *N Engl J Med* 2011; **364**: 2517–26.
43 Ishida T, Hishizawa M, Kato K *et al.* Allogeneic hematopoietic stem cell transplantation for adult T-cell leukemia-lymphoma with special emphasis on preconditioning regimen: a nationwide retrospective study. *Blood* 2012; doi: 10.1182/blood-2012-03-414490 [Epub ahead of print].

Upregulation of hsa-miR-125b in HTLV-1 asymptomatic carriers and HTLV-1-associated myelopathy/tropical spastic paraparesis patients

Larissa Deadame de Figueiredo Nicolete[1,2,3]/+, Roberto Nicolete[3], Rodrigo Haddad[2,4], Rochele Azevedo[2], Fabíola Attié de Castro[1], Yuetsu Tanaka[5], Osvaldo Massaiti Takayanagui[4], Dimas Tadeu Covas[2,4], Simone Kashima[1,2,4]

[1]Departamento de Análises Clínicas, Toxicológicas e Bromatológicas, Faculdade de Ciências Farmacêuticas de Ribeirão Preto [2]Fundação Hemocentro de Ribeirão Preto [4]Faculdade de Medicina de Ribeirão Preto, Universidade de São Paulo, Ribeirão Preto, SP, Brasil [3]Fiocruz-Rondônia, Porto Velho, RO, Brasil [5]Department of Immunology, Graduate School and Faculty of Medicine, University of the Ryukyus, Nishihara, Okinawa, Japan

The retrovirus human T lymphotropic virus type 1 (HTLV-1) promotes spastic paraparesis, adult T cell leukaemia and other diseases. Recently, some human microRNAs (miRNAs) have been described as important factors in host-virus interactions. This study compared miRNA expression in control individuals, asymptomatic HTLV-1 carriers and HTLV-1 associated myelopathy (HAM)/tropical spastic paraparesis patients. The proviral load and Tax protein expression were measured in order to characterize the patients. hsa-miR-125b expression was significantly higher in patients than in controls (p = 0.0285) or in the HAM group (p = 0.0312). Therefore, our findings suggest that miR-125b expression can be used to elucidate the mechanisms of viral replication and pathogenic processes.

Key words: HAM/TSP - hsa-miR-125b - upregulation

The retrovirus human T lymphotropic virus type 1 (HTLV-1) causes a variety of human diseases with several clinical manifestations, including adult T cell lymphoma/leukaemia (ATLL) (Poiesz et al. 1980) and HTLV-1-associated myelopathy/tropical spastic paraparesis (HAM/TSP) (Gessain et al. 1985). HTLV-1, like other retroviruses, utilises the host cellular machinery to survive and propagate. Although the gene regulatory mechanisms involving host and viral proteins have been extensively studied, data on microRNAs (miRNAs) as mediators of gene regulation in viral infections are just emerging (Scaria et al. 2006).

The roles of human miRNAs in HTLV-1 infection are beginning to be elucidated; however, previous studies were performed on patients with only ATLL or on leukaemic cell lines (Yeung et al. 2008, Bellon et al. 2009, Tomita et al. 2012), limiting the utility of these studies to one clinical manifestation characteristic of HTLV-1 infection and to cellular events characteristic of tumourigenesis, e.g., cellular proliferation and transformation. To understand whether transformation of the cell by HTLV-1 alters miRNA expression and to elucidate how miRNAs are deregulated during HTLV-1 infection, more studies examining HTLV-1 clinical manifestations are necessary. We conducted this study to address these questions. Our first aim was to quantify miRNA expression patterns that were altered in HTLV-1 asymptomatic carriers (HACs) and in patients with HAM/TSP. The second aim was to assess variations in miRNA expression and their associations with clinical conditions.

The control group (CT) in this study consisted of 21 selected blood donors. The HTLV-1 group were classified into HAC subjects (n = 10) and HAM patients (n = 13), recruited from the Neurology Department of the Hospital of the University of São Paulo, Brazil. The study was approved by the Institutional Ethical Committee of the University Hospital, Faculty of Medicine of Ribeirão Preto, University of São Paulo (process 7639/2005). All subjects gave written informed consent to participate.

Proviral load (PL) was determined according to Dehée et al. (2002). The standard used for HTLV-1 was DNA lysate from MT-2 cells (catalogue 93121518/ECACC, HPA Cultures, Salisbury, Wiltshire, UK), which contains 2.4 copies per cell of the HTLV-1 provirus. The range of the PL in the MT2 standard was 10^5-10^1 copies per reaction. The PL values were normalised to the number of copies of the β-actin gene, of which two alleles per cell were present. The total sample copy number was estimated by interpolation from the standard curve assuming one proviral copy per cell.

Peripheral blood mononuclear cells (PBMCs) from all individuals were isolated from 40 mL of total peripheral blood using a Ficoll-Paque™ density gradient (GE Healthcare, Uppsala, Uppsala län, Sweden). To quantify Tax protein by flow cytometry, at least 1 x 10^6 cells were cryopreserved in foetal calf serum (FCS) (HyClone, Logan, Utah, USA) with 10% dimethyl sulfoxide (Sigma-Aldrich, Saint Louis, Missouri, USA). To isolate RNA from PBMCs, 1 x 10^7 cells were lysed in TRIzol™ (Invitrogen Life Technologies, Carlsbad, California, USA). From the TRIzol™ RNA preparation, the lower, phenol-chloroform layer was saved and immediately after isolating the RNA protein was extracted for western blot analysis (see below).

Financial support: FAPESP (06/59388-4), CNPq, FUNDHERP
+ Corresponding author: larissanicolete@gmail.com
Received 24 November 2011
Accepted 14 March 2012

Cryopreserved cells were thawed, washed twice in phosphate buffered saline and then incubated for 12 h at 37°C, 5% CO_2 in complete medium consisting of RPMI-1640 medium (Sigma) supplemented with 10% FCS, 2 mM L-glutamine, 100 U/mL penicillin, 100 µg/mL streptomycin (Invitrogen Life Technologies) and 20 nM concanamycin (Sigma-Aldrich). After incubation, Tax protein was quantified in the cells as described by Asquith et al. (2005).

Total proteins were isolated from the TRIzol™ supernatant according to the manufacturer's protocol and a total of 30 µg was used for western blot analysis. Briefly, the proteins were transferred to polyvinylidene fluoride membranes (GE HealthCare, Chalfont St Giles, Buckinghamshire, England) and nonspecific binding sites were blocked overnight in non-fat dry-milk at 4°C. The membranes were incubated with monoclonal antibodies against Tax (Abcam, Cambridge, Massachusetts, USA) and tubulin (Santa Cruz Biotechnology, Santa Cruz, California, USA). Then, the membranes were washed with tris buffered saline-T solution and reincubated with peroxidase-conjugated secondary antibody (1:1.000; GE HealthCare, Chalfont St Giles, Buckinghamshire, England). The proteins were visualised using enhanced chemiluminescence (GE HealthCare, Chalfont St. Giles, Buckinghamshire, England).

Tax positivity in the PBMCs of HTLV-1-infected subjects, assessed by flow cytometry, was approximately 2.37%, which correlated with previous reports in the literature (Asquith et al. 2005). Due to the lack of flow cytometry samples from some subjects, distinct methods to measure Tax protein were used. To confirm if different methods could provide similar data, we used Spearman's test to determine the correlation of Tax protein expression in 11 samples. A significant p value of 0.0128 was observed. Tax protein expression was analysed to correctly classify HTLV-1 patient groups (Table) and parameters were established to assess protein expression in the follow-up of HTLV-1 patients.

The miRNAs chosen to have their expression changes in HTLV-1 patients were of the hsa-miR: 149a, 648, 221, 222, 142-5p, 26a, 29a, 374 and 125b. All of these miRNAs were chosen because they are involved in important cellular pathways. For example, Ma et al. (2011) demonstrated that miR-29 suppresses immune responses to intracellular pathogens by targeting interferon (IFN)-γ and Salvatori et al. (2011) showed that miR-26a inhibits cell cycle progression. In addition, miR-221 and miR-222 are deregulated in a number of cancers and affect the expression of cell cycle regulatory proteins (Lambeth et al. 2009). The expression of miR-142-5p is altered during T cell differentiation (Wu et al. 2007).

To analyse changes in miRNA expression, total RNA from patients and healthy controls were isolated from PBMCs by TRIzol™. Then, the RNA was quantified and 2.5 ng of RNA from each sample was reverse-transcribed (RT) using a High-Capacity cDNA Archive Kit (Applied Biosystems, Foster City, California, USA). Stem-loop RT primers specific for each miRNA were used in the RT-polymerase chain reaction (PCR) (Chen et al. 2005). Mature miRNAs were quantified using the TaqMan MicroRNA Assay (Applied Biosystems, Foster City, California, USA) according to the manufacturer's protocol. Quantitative PCR was used to quantify the abundance of the RT-PCR products; results from all PBMC samples were normalised to the geometric mean result from three different small nucleolar RNAs (RNU 24, RNU48 and RNU43). Relative mRNA abundance was quantified using the $2^{-\Delta\Delta Ct}$ method. To assess expression of miRNAs, the Mann-Whitney U-test was used to compare patients vs. healthy donors. To compare control individuals vs. HAC and to compare control vs. HAM, the Kruskal-Wallis test was performed followed by Dunn's post-test. The Spearman test was employed to evaluate the correlations between provirus copy number and microRNA expression.

Of all miRNAs tested, miR-125b was the only miRNA that presented significant expression variation amongst the three groups. hsa-miR-125b expression was

TABLE

Human T lymphotropic virus type 1 (HTLV-1) patients characterization

Sample	Gender	Age (years)	Proviral load	Tax protein	
				Western	Flow cytometry
HAC 01	F	52	50.96	0.80	ND
HAC12	F	51	491.94	1.36	ND
HAC13	F	42	ND	2.01	ND
HAC15	M	53	ND	1.11	ND
HAC16	F	55	ND	0.40	0.87
HAC19	F	33	233.88	0.21	0.48
HAC20	M	45	224.96	1.94	ND
HAC21	M	46	ND	0.61	4.12
HAC22	M	61	0.00	0.52	ND
HAC23	F	46	0.00	0.08	0.53
HAM01	F	55	368.18	1.00	1.20
HAM02	F	34	1.233.97	2.76	ND
HAM05	F	61	3.296.98	0.81	3.39
HAM08	M	47	1.090.20	0.97	ND
HAM09	M	64	775.40	0.64	4.56
HAM13	F	49	303.78	1.16	ND
HAM14	F	61	ND	0.67	4.21
HAM15	F	62	1.323.84	ND	ND
HAM16	M	54	0.00	0.14	1.15
HAM17	F	55	42.07	0.24	1.09
HAM18	F	48	ND	0.58	2.75
HAM19	F	42	2.068.97	1.09	ND

the analyses (western vs. flow cytometry) were evaluated by Spearman's test (p = 0.0128). The correlation was applied due to the lack of cells to be evaluated by flow cytometry (the preferential method). HAC: HTLV-1 asymptomatic carrier; HAM: HTLV-1 associated myelopathy/tropical spastic paraparesis; ND: not determined.

significantly higher in patients than controls (p = 0.0285) (A in Figure). When the groups were re-analysed after classifying by clinical condition (Tax protein level), hsa-miR-125b presented a progressive increase in expression from CT to HAC to HAM (p = 0.0312) (B in Figure). Our findings show that hsa-miR-125b expression increased in HTLV-1 carriers and HAM patients; however, the Spearman correlations of hsa-miR-125b expression with PL and Tax expression did not suggest any statistical significance (data not shown). It is possible that host factors, which can be involved in miR-125b deregulation, contributed to the absence of statistically significant correlations between miR-125b expression and HTLV-1 infection.

The viral protein Tax is capable of inactivating p53 and compromising several cellular events (Taylor & Nicot 2008). Recently Le et al. (2011) demonstrated that miR-125b is responsible for regulating 20 novel targets in the p53 pathway. Therefore, it is reasonable to believe that some deregulation of miRNA expression could be correlated with p53 inactivation. Rossi et al. (2011) demonstrated that during the transformation of naïve $TCD4^+$ to effector memory cells, miR-125b expression significantly decreases. When this miRNA is added exogenously into $TCD4^+$ cells, they secrete less IFN-γ and express interleukin-2Rβ, suggesting that high expression of miR-125b inhibits the secretion of IFN-γ by $TCD4^+$ effector cells. Additionally, Rajaram et al. (2011) demonstrated that miR-125b is responsible for reducing the production of TNF-α in infected macrophages when the macrophages are activated to produce TNF-α in a model of tuberculosis.

In patients with HTLV-1, especially patients with an enhanced inflammatory response, both TNF-α and IFN-γ secretion are increased (Yamana et al. 2009). While further studies will be crucial to elucidate if miR-125b is increased in virus carriers, miR-125b expression should be assessed in HAM/TSP patients, as an increase in expression may result from a host's attempt to control the production of TNF-α and IFN-γ. Experiments correlating miR-125b expression with TNF-α, IFN-γ and/or p53 levels may also be important for elucidating the mechanism by which certain patient populations develop myelopathy. Furthermore, assessing miR-125b expression in patients over a time course, for example, in the follow-up of HAC patients, could determine if the level of miR-125b can be used as a diagnostic marker.

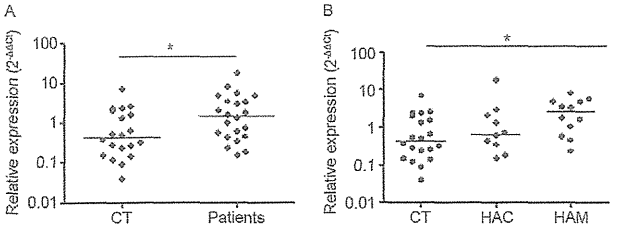

A: hsa-miR-125b expression in control individuals (CT) and patients (p = 0.0285) by Mann-Whitney analysis. Horizontal bars represent median values of which group (CT = 1.15; patients = 2.84); B: hsa-miR-125b expression among CT, asymptomatic carriers (HAC) and human T lymphotropic virus type 1-associated myelopathy/tropical spastic paraparesis (HAM/TSP) patients (HAM) (p = 0.0312). Horizontal bars represent median values of which group by Kruskall-Wallis analysis (CT = 1.152; HAC = 2.652; HAM = 2.99).

In conclusion, we suggest that further studies analysing the miRNAs that exhibit altered expression patterns in HAM/TSP will likely enhance our understanding of how miRNAs participate in the progression of myelopathy and will open avenues for new therapeutic approaches.

ACKNOWLEDGEMENTS

To Tathiane Maistro Malta, for providing technical support in some experiments.

REFERENCES

Asquith B, Mosley AJ, Heaps, A, Tanaka Y, Taylor GP, Mclean AR, Bangham CR 2005. Quantification of the virus-host interaction in human T lymphotropic virus I infection. *Retrovirol 2*: 1-9.

Bellon M, Lepelletier Y, Hermine O, Nicot C 2009. Deregulation of microRNA involved in hematopoiesis and the immune response in HTLV-I adult T-cell leukemia. *Blood 113*: 4914-4917.

Chen C, Ridzon DA, Broomer AJ, Zhou Z, Lee DH, Nguyen JT, Barbisin M, Xu NL 2005. Real-time quantification of microRNAs by stem-loop RT-PCR. *Nucleic Acids Res 33*: e179.

Dehée A, Césaire R, Désiré N, Lézin A, Bourdonné O, Béra O, Plumelle Y, Smadja D, Nicolas JC 2002. Quantitation of HTLV-I proviral load by a TaqMan real-time PCR assay. *J Virol Methods 102*: 37-51.

Gessain A, Barin F, Vernant JC, Gout O, Maurs L, Calender A, De The G 1985. Antibodies to human T-lymphotropic virus type-I in patients with tropical spastic paraparesis. *Lancet II*: 407-409.

Lambeth LS, Yao Y, Smith LP, Zhao Y, Nair V 2009. MicroRNAs 221 and 222 target p27Kip1 in Marek's disease virus-transformed tumour cell line MSB-1. *J Gen Virol 90*: 1164-1171.

Le MT, Shyh-Chang N, Khaw SL, Chin L, Teh C, Tay J, O'Day E, Korzh V, Yang H, Lal A 2011. Conserved regulation of p53 network dosage by microRNA-125b occurs through evolving miRNA-target gene pairs. *PLoS Genet 7*: e1002242.

Ma F, Xu S, Liu X, Zhang Q, Xu X, Liu M, Hua M, Li N, Yao H, Cao X 2011. The microRNA miR-29 controls innate and adaptive immune responses to intracellular bacterial infection by targeting interferon-γ. *Nat Immunol 12*: 861-869.

Poiesz BJ, Ruscetti FW, Gazdar AF, Bunn PA, Minna JD, Gallo RC 1980. Detection and isolation of type C retrovirus particles from fresh and cultured lymphocytes of a patient with cutaneous T-cell lymphoma. *Proc Natl Acad Sci USA 77*: 7415-7419.

Rajaram MV, Ni B, Morris JD, Brooks MN, Carlson TK, Bakthavachalu B, Schoenberg DR 2011. Mycobacterium tuberculosis lipomannan blocks TNF biosynthesis by regulating macrophage MAPK-activated protein kinase 2 (MK2) and microRNA miR-125b. *Proc Natl Acad Sci USA 108*: 17408-17413.

Rossi RL, Rossetti G, Wenandy L, Curti S, Ripamonti A, Bonnal RJ, Birolo RS, Moro M 2011. Distinct microRNA signatures in human lymphocyte subsets and enforcement of the naive state in $CD4^+$ T cells by the microRNA miR-125b. *Nat Immunol 12*: 796-803.

Salvatori B, Iosue I, Djodji Damas N, Mangiavacchi A, Chiaretti S, Messina M 2011. Critical role of c-Myc in Acute myeloid leukemia involving direct regulation of miR-26a and histone methyltransferase EZH2. *Genes Cancer 2*: 585-592.

Scaria V, Hariharan M, Maiti S, Pillai B, Brahmachari SK 2006. Host-virus interaction: a new role for microRNAs. *Retrovirol 3*: 1-9.

Taylor JM, Nicot C 2008. HTLV-1 and apoptosis: role in cellular transformation and recent advances in therapeutic approaches. *Apoptosis 13*: 733-747.

Tomita M, Tanaka Y, Mori N 2012. MicroRNA miR-146a is induced by HTLV-1 tax and increases the growth of HTLV-1-infected T-cells. *Int J Cancer 130*: 2300-2309.

Wu H, Neilson JR, Kumar P, Manocha M, Shankar P, Sharp PA, Manjunath N 2007. miRNA profiling of naïve, effector and memory CD8 T cells. *PLoS ONE 2*: e1020.

Yamana Y, Araya N, Sato T, Utsunomiya A, Azakami K, Hasegawa D, Izumi T, Fujita H 2009. Abnormally high levels of virus-infected IFN-gamma$^+$ CCR4$^+$ CD4$^+$ CD25$^+$ T cells in a retrovirus-associated neuroinflammatory disorder. *PLoS ONE 4*: e6517.

Yeung ML, Yasunaga J, Bennasser Y, Dusetti N, Harris D, Ahmad N, Matsuoka M, Jeang KT 2008. Roles for microRNAs, miR-93 and miR-130b and tumor protein 53-induced nuclear protein 1 tumor suppressor in cell growth dysregulation by human T-cell lymphotrophic virus 1. *Cancer Res 68*: 8976-8985.

JSHC
Japan Society of
Histochemistry and Cytochemistry
Established 1959

Acta Histochem. Cytochem. 45 (2): 83–106, 2012
doi:10.1267/ahc.11034

Review

Development of Ultra-Super Sensitive Immunohistochemistry and Its Application to the Etiological Study of Adult T-Cell Leukemia/Lymphoma

Kazuhisa Hasui[1], Jia Wang[1,5], Yuetsu Tanaka[2], Shuji Izumo[3], Yoshito Eizuru[4] and Takami Matsuyama[1]

[1]Division of Immunology, Department of Infection and Immunity, Institute Research Center (Health Research Course), Kagoshima University Graduate School of Medical and Dental Sciences, [2]Department of Immunology, Graduate School of Medicine, University of the Ryukyus, [3]Chronic Viral Diseases Div. of Molecular Pathology, Center for Chronic Viral Diseases (Infection and Immunity), Institute Research Center (Health Research Course), Kagoshima University Graduate School of Medical and Dental Sciences, [4]Chronic Viral Diseases Div. of Persistent & Oncogenic Viruses, Center for Chronic Viral Diseases (Infection and Immunity), Institute Research Center (Health Research Course), Kagoshima University Graduate School of Medical and Dental Sciences and [5]Present address: INAMORI Frontier Research Center, Kyushu University, 744 Motooka, Nishi-ku, Fukuoka 819–0395, Japan

Received July 15, 2011; accepted February 14, 2012; published online April 21, 2012

Antigen retrieval (AR) and ultra-super sensitive immunohistochemistry (ultra-IHC) have been established for application to archival human pathology specimens. The original ultra-IHC was the ImmunoMax method or the catalyzed signal amplification system (ImmunoMax/CSA method), comprising the streptavidin-biotin complex (sABC) method and catalyzed reporter deposition (CARD) reaction with visualization of its deposition. By introducing procedures to diminish non-specific staining in the original ultra-IHC method, we developed the modified ImmunoMax/CSA method with AR heating sections in an AR solution (heating-AR). The heating-AR and modified ImmunoMax/CSA method visualized expression of the predominantly simple present form of HTLV-1 proviral DNA pX region p40Tax protein (Tax) in adult T-cell leukemia/lymphoma (ATLL) cells in archival pathology specimens in approximately 75% of cases. The simple present form of Tax detected exhibited a close relation with ATLL cell proliferation. We also established a new simplified CSA (nsCSA) system by replacing the sABC method with the secondary antibody- and horse radish peroxidase-labeled polymer reagent method, introducing the pretreatments blocking non-specific binding of secondary antibody reagent, and diminishing the diffusion of deposition in the CARD reaction. Combined with AR treating sections with proteinase K solution (enzymatic-AR), the nsCSA system visualized granular immunostaining of the complex present form of Tax in a small number of ATLL cells in most cases, presenting the possibility of etiological pathological diagnosis of ATLL and suggesting that the complex present form of Tax-positive ATLL cells were young cells derived from ATLL stem cells. The heating-AR and ultra-IHC detected physiological expression of the p53 protein and its probable phosphorylation by Tax in peripheral blood mononuclear cells of peripheral blood tissue specimens from HTLV-1 carriers, as well as physiological and pathological expression of the molecules involved with G1 phase progression and G1–S phase transition (E2F-1, E2F-4, DP-1, and cyclin E) in ATLL and peripheral T-cell lymphoma cells. The ultra-IHC with AR is useful for etiological pathological diagnosis of ATLL since HTLV-1 pathogenicity depends on that of Tax, and can be a useful tool for studies translating advanced molecular biology and pathology to human pathology.

Key words: ultra-super sensitive immunohistochemistry, HTLV-1, p53 protein, cell cycle, adult T-cell leukemia/lymphoma (ATLL)

Correspondence to: Dr. Kazuhisa Hasui, Division of Immunology, Department of Infection and Immunity, Institute Research Center (Health Research Course), Kagoshima University Graduate School of Medical and Dental Sciences, Sakuragaoka 8–35–1, Kagoshima 890–8544, Japan. E-mail: anahasui@m3.kufm.kasgoshima-u.ac.jp

I. Introduction

Adult T-cell leukemia/lymphoma (ATLL) is a type of peripheral T-cell leukemia/lymphoma (PTCL) that is caused

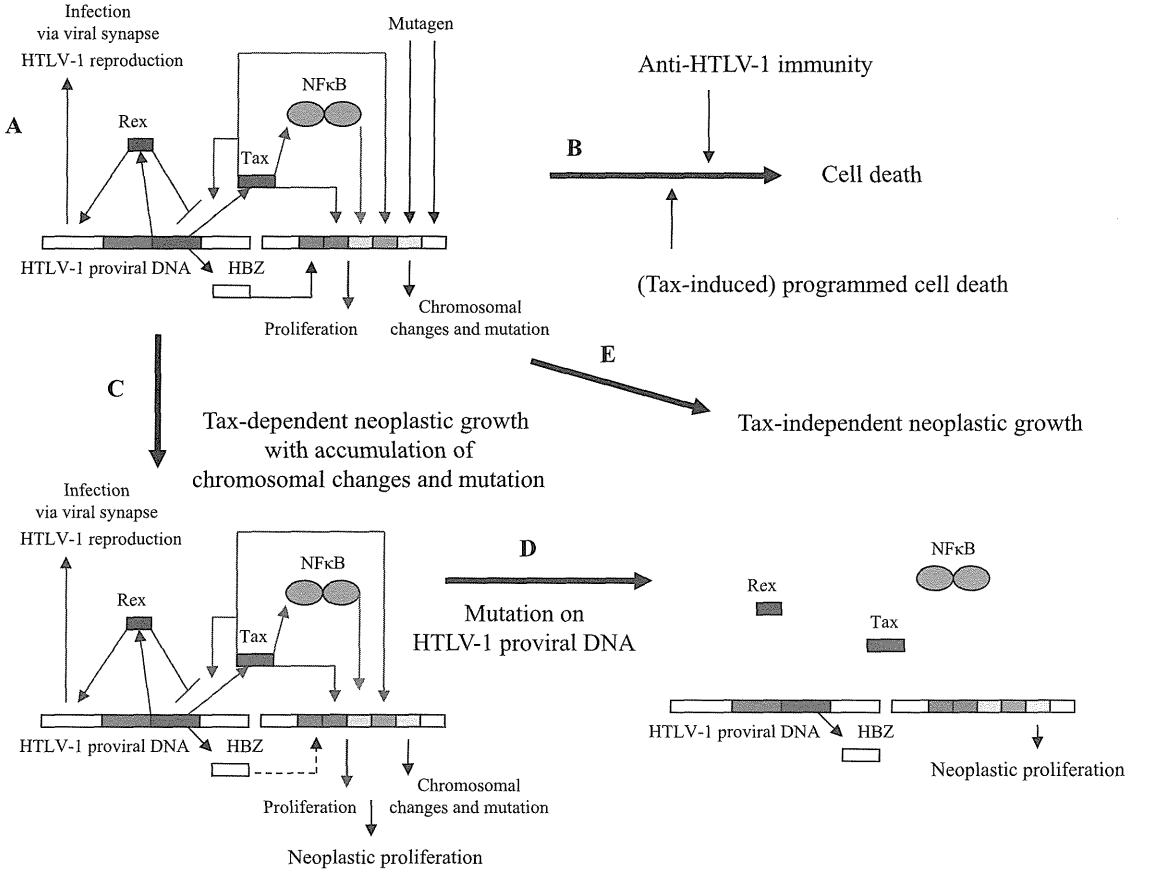

Fig. 1. Pathogenicity of human T-lymphotropic virus type 1 (HTLV-1). ATLL is thought to be caused by pathogenicity of the HTLV-1 proviral DNA pX region p40Tax protein (Tax) and effects of external and internal mutagens. Recently, HTLV-1 basic leucine zipper (HBZ) mRNA from the HTLV-1 proviral DNA minus strand is regarded to cause ATLL independently of Tax. **A**) Latent phase HTLV-1 infection: Tax synthesis is modulated by HTLV-proviral DNA pX region p27Rex protein (Rex). Tax trans-activates and -suppresses host cell genes. HBZ mRNA propels proliferation of the host cells through E2F-1 signaling to the cell cycle. Internal and external mutagens affect host cell genes when APOBEC3G is one of the internal mutagens in activated T-cells. **B**) Anti-HTLV-1 immunity: Anti-HTLV-1 immunity would eliminate HTLV-1 infected T-cells. **C**) Early phase ATLL: Neoplastic proliferation of early ATLL cells depends on Tax in the background of the effects of HBZ mRNA, chromosomal changes and mutations. **D**) Late phase ATLL: Accumulation of chromosomal changes and mutations with and without the effects of Tax, APOBEC3G and the other mutagens confer neoplastic properties to early phase ATLL cells. Tax may disappear and its DNA might be destroyed in most late phase ATLL cells. **E**) Development of a Tax-independent T-cell neoplasm: Depending on the chromosomal changes and mutations induced by the external and internal mutagens and possibly by HBZ mRNA, HTLV-1 infected T-cells may develop into a Tax-independent T-cell neoplasm.

by human T-lymphotropic virus type 1 (HTLV-1) [96]. ATLL occurs in the lifetime of 2 to 5% of HTLV-1 carriers [4]. ATLL is subcategorized clinically into smoldering, including cutaneous type, chronic and acute leukemia, and lymphoma types [89]. Most ATLL patients have anti-HTLV-1 antibodies [36] when ATLL cells exhibit monoclonal integration of HTLV-1 proviral DNA [109, 111].

In the natural history of HTLV-1 infection, following latent infection spanning more than 30 years from the initial infection in the perinatal period (Fig. 1) and based on virological, molecular biological and immunological understanding of HTLV-1 infection, early-phase ATLL cells with neoplastic properties dependent on the HTLV-1 proviral DNA pX region p40Tax protein (Tax) [42, 70, 80, 93, 101, 110] appear under the effects of external and internal mutagens [19, 76, 84] following the accumulation of mutations induced by repeated Tax expression [18] in the background of persistent proliferation of HTLV-1-infected T-cells, which is probably induced by HTLV-1 basic leucine zipper (HBZ) mRNA [64, 65]. Then, late-phase ATLL cells with neoplastic properties independent of Tax appear when mutation has progressed in the host cell DNA and HTLV-1 proviral DNA including pX p40Tax DNA sequence [19].

ATLL cells exhibit the $CD4^+$ $CD25^+$ forkhead box protein $P3^+$ ($Foxp3^+$) phenotype of regulatory T-cells [108]. PTCL in a patient with anti-HTLV-1 antibodies or with clinicopathological information of HTLV-1 proviral DNA integration is diagnosed practically as ATLL. On the other hand, etiological pathological diagnosis of ATLL is expected based on immunohistochemistry (IHC) detecting of

A. Super sensitive IHC (ordinary-IHC) methods related to ultra-IHC

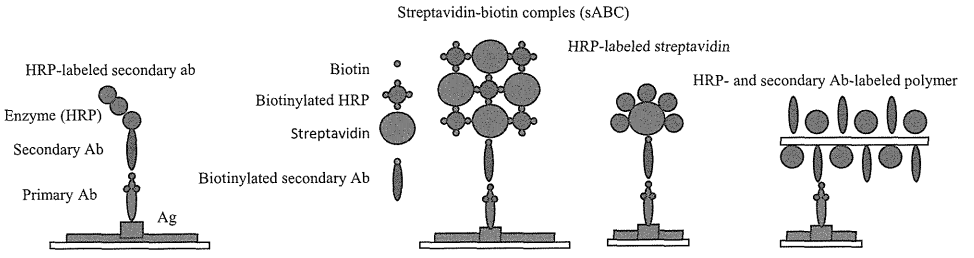

a) Enzyme-labeled secondary antibody method **b) ABC(sABC) method** **c) LSAB method** **d) Polymer method**

B. Ultra-IHC by means of CARD reaction

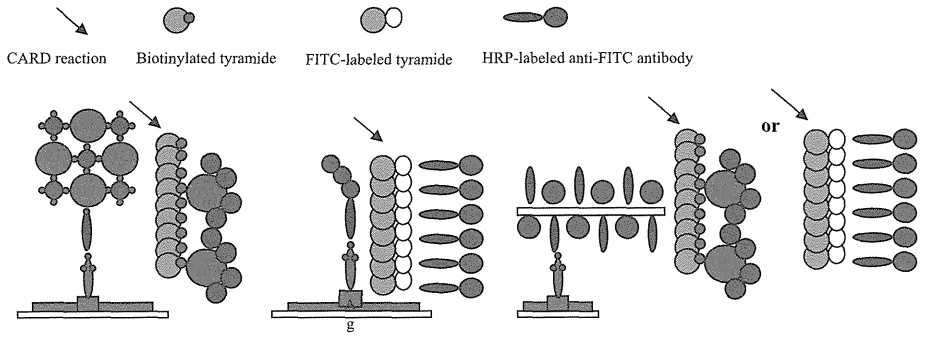

e) ImmunoMax/CSA method **f) Dako CSA II system** **g) New simplified CSA system**

C. Pretreatments for ultra-IHC by means of CARD reaction

	Pretreatment				
	Inactivation of endogenous peroxidase	Suppression of non-specific staining of primary antibody	Masking of endogenous biotin	Suppression of non-specific staining of secondary antibody	Suppression of non-specific staining in CARD reaction
Original ImmunoMax/CSA method	○	○	-	-	-
Modified ImmunoMax/CSA method	○ **(2 times)**	○	○	-	-
Dako CSA II system	○	○	-	-	-
New simplified CSA system	○ **(2 times)**	○	-	○	○

Fig. 2. Products of super and ultra-super sensitive immunohistochemistry (IHC) and pretreatments for ultra-super sensitive IHC (ultra-IHC). Differences among enzyme-labeled antibody indirect methods can be observed in their products and in each method's pretreatments. **A**) Super sensitive IHC (ordinary-IHC) methods related to ultra-IHC are **a**) classic enzyme-labeled secondary antibody method, **b**) avidin (streptavidin)-biotin complex method (ABC/sABC method), **c**) horse radish peroxidase (HRP)-labeled streptavidin-biotin complex method (LSAB method, and **d**) HRP- and secondary antibody-labeled polymer reagent method (Polymer method). **B**) Ultra-IHC by means of catalyzed reporter deposition (CARD) reaction. The original ImmunoMax/CSA method (**e**) comprises the sABC method (**b**) and a CARD reaction with detection of deposited biotinylated tyramide by the LSAB method (**c**). Dako CSA II system (**f**), a biotin-free system, comprises the enzyme-labeled secondary antibody method (**a**) and CARD reaction with detection of deposited FITC-labeled tyramide with HRP-labeled anti-FITC antibody. The new simplified CSA system (**g**) comprises the polymer method and CARD reaction with detection of deposited biotinylated tyramide by the LSAB method (**c**) or with detection of deposited FITC-labeled tyramide with HRP-labeled anti-FITC antibody. **C**) Pretreatment for ultra-IHC with the CARD reaction. The original ImmunoMax/CSA method is equipped with pretreatments for endogenous peroxidase and non-specific binding of the primary antibody. The modified ImmunoMax/CSA method introduces masking of endogenous biotin in itself. The Dako CSA II system is not equipped with additional pretreatments besides those available in the original ImmunoMax/CSA method. The new simplified CSA system is equipped with additional pretreatments for non-specific binding of the secondary antibody and non-specific staining in CARD reaction.

Tax, HTLV-1 proviral DNA pX p27Rex protein (Rex) and HBZ mRNA/protein in PTCL cells. However, the amount of Tax, Rex and HBZ protein in ATLL cells is too small to be detected by ordinary super sensitive enzyme-labeled antibody methods of IHC (ordinary-IHC) such as avidin/streptavidin-biotin complex (ABC/sABC, Fig. 2b), labeled streptavidin-biotin complex method (LSAB, Fig. 2c), and polymer methods (Fig. 2d). Therefore, these proteins should be detected by ultra-super sensitive IHC (ultra-IHC) comprising an indirect enzyme-labeled antibody method and catalyzed reporter deposition (CARD) reaction (Fig. 2e). Some ultra-IHC kits are commercially available but suffer from strong non-specific staining. We have succeeded in developing ultra-IHC of Tax and Rex on routine paraffin sections of ATLL [30, 31, 35, 62], solving the problems that cause the strong non-specific staining.

This review describes our development of the ultra-IHC and its application, which employs anti-HTLV-1-related antibodies, to the pathological diagnosis of ATLL and the analysis of ATLL oncogenesis and pathogenesis.

II. Development of Ultra-IHC

Antigen retrieval (AR) heating sections in an AR solution such as 0.01 M citrate buffer, pH 6.0 (heating-AR) heralded the era of so-called paraffin section IHC in the 1990s [86–88]. Currently, many antigens can be detected in archival human pathology specimens by combining heating-AR with ordinary-IHC. In ultra-IHC, heating-AR retrieves larger amounts of antigen based on autoclaving (121°C for 5 min), pressure cooking (for 10 min after boiling) and microwaving (3 times heating for 1 min) but also yields more non-specific staining, whereas heating-AR in 4 M urea solution demonstrated less non-specific staining than heating in 0.01 M citrate buffer [27, 30]. Since the J chain in immunoglobulins A and M and amyloid protein are unmasked by rinsing sections in a solution of highly concentrated denaturing reagent such as urea at 4°C overnight [17, 71], the heating-AR in 4 M urea is also expected to denature and expose antigens to the antibody. Recently, heating-AR has often been performed independently of the AR solution pH [104]. On the other hand, AR treating sections with an enzyme such as proteinase K (enzymatic-AR) is expected to enable visualization of molecules that form complexes or bind with other proteins and DNA, etc. by partly digesting the molecule/tissue complexes obscuring the target molecules [50].

Ultra-IHC was introduced in the field of surgical pathology as the original ImmunoMax/CSA method [67] (Fig. 2e), comprising heating-AR, sABC method (Fig. 2b), CARD reaction (Fig. 2B) and detection of the CARD deposition by LSAB method (Fig. 2c). The ImmunoMax method employed serum solutions such as phosphate buffer saline (PBS) containing 8% horse serum or 8% human AB type serum for blocking non-specific binding (Protein block) of the primary antibody, while CSA system used a serum-free solution such as PBS containing 0.25% casein

Table 1. *Protocols of ultra-super sensitive immunohistochemistry*

A) Protocol of modified ImmunoMax/Catalyzed signal amplification (CSA) method

Step	Work
a	Deparaffinization.
b	First inactivation of endogenous peroxidase (IEP) rinsing sections in methanol containing 0.3% H_2O_2 for 20 min.
c	Antigen retrieval
d	Rinse sections in phosphate buffer saline (PBS).
	Set slides to the autostainer.
1	Second IEP rinsing sections in PBS containing 3% H_2O_2 for 5 min.
2–4	3 times Rinse1
5	*Protein block suppressing non-specific binding of primary antibody for 5 min.
6	**Primary antibody reaction** for 15 min.
7–9	3 times Rinse1
10	Endogenous biotin mask (1) rinsing in avidin solution for 15 min.
11–13	3 times Rinse1
14	Endogenous biotin mask (2) rinsing in biotin solution for 15 min.
15–17	3 times Rinse1
18	**Protein block suppressing non-specific binding of secondary antibody for 5 min.
19	**Biotinylated secondary antibody reaction** for 15 min.
20–22	3 times Rinse1
23	**Horse radish peroxidase (HRP)-labeled streptavidin reaction** for 15 min.
24–26	3 times Rinse1
27	***Protein block suppressing diffusion of catalyzed tyramide in the Catalyzed reporter deposition (CARD) reaction for 1 min.
28	**CARD reaction** for 15 min.
29–30	2 times Rinse2
31	**HRP-labeled streptavidin reaction** for 15 min
32–33	2 times Rinse2
34	**H_2O_2-Diaminobenzidine (DAB) reaction** for 5 min.
35	Rinse with distilled water to stop the DAB reaction.
36	Counterstaining of nuclei
37	Rinse with distilled water.
	Remove slides from the autostainer.
	Dehydrate slides and mount section with plastic medium.

Rinse1: Rinse with Tris buffer saline containing 0.1% Tween 20 (TBST) warmed at 35°C.
Rinse2: Rinse with TBST warmed at 35°C. But the rinsing buffer is PBS at room temperature in a case when a rinsing buffer can be changed by a semi-autostainer (MicroProbe™, Fisher Scientific Co.).
*: Protein block employs PBS containing 0.25% casein (Dako) with 8% horse serum.
**: Protein block employs PBS containing 0.25% casein (Dako) with 8% goat serum.
***: Protein block employs PBS containing 0.25% casein (Dako) or PBS with 3% BSA.
Steps 18 and 27 were inserted according to the new simplified CSA system (Table 1C).

Table 1. Continued (1).

B) The protocol of Dako CSA II system, modified according to new simplified CSA system

Step	Work
a	Deparaffinization.
b	Antigen retrieval
c	Rinse sections in PBS

Set slides to the autostainer.

1	inactivation of endogenous peroxidase rinsing sections in methanol containing 0.3% H_2O_2 for 20 min.
2–4	3 times Rinse1
5	*Protein block for 5 min.
6	**Primary antibody reaction** for 15 min.
7–9	3 times Rinse1
10	**Protein block for 5 min.
11	**HRP-labeled secondary antibody reaction** for 15 min.
12–14	3 times Rinse1
15	***Protein block for 1 to 5 min.
16	**CARD reaction of fluorescein isothiocyanate (FITC)-labeled tyramide** for 30 min.
17–18	2 times Rinse2
19	**HRP-labeled anti-FITC antibody reaction** for 30 min.
20–21	2 times Rinse2
22	**H_2O_2-DAB reaction** for 5 min.
23	Rinse with distilled water to stop the DAB reaction.
24	Counterstaining of nuclei
25	Rinse with distilled water.

Remove slides from the autostainer.

Dehydrate slides and mount section with plastic medium.

Steps 10 and 15 are inserted according to the new simplified CSA system (Table 1C).
Rinse1: Rinse with Tris buffer saline containing 0.1% Tween 20 (TBST) warmed at 35°C.
Rinse2: Rinse with TBST warmed at 35°C. But the rinsing buffer is PBS at room temperature in a case when a rinsing buffer can be changed by a semi-autostainer (MicroProbe™, Fisher Scientific Co.).
Rinse: Post-reaction wash with TBST at room temperature.
*: Protein block employs PBS containing 0.25% casein (Dako) with 8% horse serum.
**: Protein block employs PBS containing 0.25% casein (Dako) with 8% goat serum.
***: Protein block suppresses diffusion of depositing FITC-labeled tyramide in the CARD reaction, pre-treating sections with PBS containing 3% polyethylene glycol (PEG) #20000 and 0.1% Tween 20 or with PBS containing 0.3% BSA and 0.1% Tween 20.

for Protein block. As molecular biology developed, the amounts of molecules traditionally targeted by IHC, such as those of signal transduction molecules and phosphorylated functional proteins, became too minute to be visualized by ordinary-IHC. Then, the ultra-IHC was expected to detect much smaller amounts of molecules, amplifying the ordinary-IHC signals a thousand times through the CARD reaction.

Unfortunately, the original ImmunoMax/CSA method required 2 times horse-radish peroxidase (HRP) reaction in

Table 1. Continued (2).

C) New simplified CSA system (nsCSA system)

Step	Work
a	Deparaffinization.
b	First inactivation of endogenous peroxidase (IEP) rinsing sections in methanol containing 0.3% H_2O_2 for 20 min.
c	Antigen retrieval
d	Rinse sections in PBS

Set slides to the autostainer.

1	Second IEP rinsing sections in PBS containing 3% H_2O_2 for 5 min.
2–4	3 times Rinse1
5	*Protein block for 5 min.
6	**Primary antibody reaction** for 15 min.
7–9	3 times Rinse1
10	**Protein block for 5 min.
11	**HRP- and secondary antibody-labeled polymer reagent reaction** for 15 min.
12–14	3 times Rinse1 (Go to step15)
15	***Protein block for 1 min.
16	**CARD reaction of biotinylated tyramide** for 15 min.
17–18	2 times Rinse2
19	**HRP-labeled streptavidin reaction** for 15 min.
20–21	2 times Rinse2 (Go to step 22)

In a case employing FITC-labeled tyramide.

15	****Protein block for 1 min.
16	**CARD reaction of FITC-labeled tyramide** for 30 min.
17–18	2 times Rinse2
19	**HRP-labeled anti-FITC antibody reaction** for 30 min.
20–21	2 times Rinse2 (Go to step 22)
22	**H_2O_2-DAB reaction** for 5 min.
23	Rinse with distilled water to stop the DAB reaction.
24	Counterstaining of nuclei
25	Rinse with distilled water.

Remove slides from the autostainer.

Dehydrate slide and mount section with plastic medium.

Rinse1: Rinse with Tris buffer saline containing 0.1% Tween 20 (TBST) warmed at 35°C.
Rinse2: Rinse with TBST warmed at 35°C. But the rinsing buffer is PBS at room temperature in a case when a rinsing buffer can be changed by a semi-autostainer (MicroProbe™, Fisher Scientific Co.).
*Protein block: Protein block suppresses non-specific binding of primary antibody, rinsing sections in PBS containing 0.25% casein (Dako) with 8% horse serum or in PBS containing 3% BSA and 8% horse or goat serum
**Protein block: Protein block suppresses non-specific binding of secondary antibody, rinsing sections in PBS containing 0.25% casein (Dako) with 8% goat serum or in PBS containing 3% BSA and 8% goat serum.
***Protein block: Protein block suppresses diffusion of depositing biotinylated tyramide in the CARD reaction, pre-treating sections with PBS containing 0.25% casein (Dako) or PBS with 3% BSA.
****Protein block: Protein block suppresses diffusion of depositing FITC-labeled tyramide in the CARD reaction, pre-treating sections with PBS containing 3% polyethylene glycol (PEG) #20000 and 0.1% Tween 20 or with PBS containing 0.3% BSA and 0.1% Tween 20.

the CARD reaction and diaminobenzidine (DAB)-H_2O_2 reaction for visualization and 2 times biotin-streptavidin binding reaction in the sABC method and in the LSAB method detecting deposited catalyzed tyramide. Moreover, its post-reaction wash appeared incomplete. Therefore, the original ImmunoMax/CSA method (Fig. 2C, Original ImmunoMax/CSA method) amplified an extremely low level of residual activity of endogenous peroxidase, a rather small amount of endogenous biotin, and a trace level of residual reaction reagents into a huge amount of non-specific staining. Thus, the modified ImmunoMax/CSA method (Table 1A) was designed [30] to diminish non-specific staining by introducing double inactivation of endogenous peroxidase before and after AR, endogenous biotin mask treating sections with avidin and biotin solutions between the primary antibody and biotinylated secondary antibody reactions (Fig. 2C, Modified ImmunoMax/CSA method), and the post-reaction wash (PR wash) 3 times in Tris-buffered saline containing 0.5% Tween 20 (TBST) warmed to 35°C [30]. The modified ImmunoMax/CSA method employed PBS containing 8% horse serum and 0.25% casein for Protein block before the primary antibody reaction. Biotinylated tyramide deposited in the CARD reaction was washed out by rinsing 3 times in the warmed TBST so the PR wash following the CARD reaction was defined as rinse twice in PBS at room temperature when the PR wash solution could be changed [30]. Finally, the modified ImmunoMax/CSA method comprised 37 steps in an autostainer (Table 1A), where 2 steps of Protein block for the secondary antibody reaction (step 18, Table 1A) and pretreatment for the reaction (step 27, Table 1A) were those employed in the new simplified CSA (nsCSA) system (Table 1C).

However, non-specific staining persisted somewhat in the modified ImmunoMax/CSA method, and varied with each case. The positive staining of the modified ImmunoMax/CSA method was evaluated in comparison with staining performed without the primary antibody reaction (negative control staining). To prevent non-specific staining caused by endogenous biotin, Dako supplied a CSA II system (Table 1B) to replace the sABC method (Fig. 2b) and the biotinylated tyramide-CARD reaction with HRP-labeled secondary antibody method (Fig. 2a) and the fluorescein isothiocyanate (FITC)-labeled tyramide-CARD reaction (Fig. 2f) but did not equip the Protein block to suppress non-specific binding of the secondary antibody and the pretreatment to suppress the diffusion of catalyzed FITC-labeled tyramide (Fig. 2C, Dako CSA II system). Then, non-specific background staining with the Dako CSA II system was quite high. On the other hand, we developed new simplified CSA system (nsCSA system) (Table 1C, Fig. 2g), replacing the sABC method (Fig. 2b) with the HRP- and secondary antibody-labeled polymer reagent method (Fig. 2d), where additional Protein block suppressed non-specific binding of the polymer reagent and pretreatment suppressed diffusion of the catalyzed biotinylated or FITC-labeled tyramide (Fig. 2C, new simplified CSA system) [28, 34].

The reagent for the Protein block was PBS containing 0.25% casein or 3% bovine serum albumin (BSA), diminishing non-specific staining of the primary antibody and polymer reagents in the nsCSA system [28, 34]. It may have been because the blocking reagent can mask most non-specific binding sites, whereas competitive blocking by the blocking reagent in the primary antibody and polymer reagents would mask approximately half of all non-specific binding sites. Catalyzed tyramide rarely diffused to be deposited in areas distant from CARD reaction sites. Pretreatment with biochemically inactive molecules was required to achieve deposition of catalyzed tyramide much nearer to the CARD reaction sites. The pretreatment reagent was PBS containing 0.25% casein or PBS containing 3% BSA and 0.1% Tween 20 for the biotinylated tyramide-CARD reaction, while PBS containing 3% polyethylene glycol (PEG) #20000 and 0.1% Tween 20 or PBS containing 0.3% BSA and 0.1% Tween 20 was employed for the FITC-labeled tyramide-CARD reaction [28]. The nsCSA system of the biotinylated tyramide-CARD reaction was free from non-specific staining of endogenous biotin even in endogenous biotin-rich tissue such as that from the liver [28]. Antigen detection sensitivity was high in the following order: nsCSA system with the biotinylated tyramide-CARD reaction (Table 1C), nsCSA system with the FITC-labeled tyramide-CARD reaction (Table 1C), and the Dako CSA II system (Table 1B) with pretreatments diminishing non-specific staining according to nsCSA system [28] because the polymer reagent method (Fig. 2d) in the nsCSA system was more sensitive than that of the HRP-labeled secondary antibody method (Fig. 2a) in the CSA II system.

Protein block (PBS containing 0.25% casein, Dako) was a powerful reagent in the nsCSA system but the procedure, which exceeded 15 min, prevented antigen-antibody reaction, whereas PBS containing 3% BSA did not [28]. However, ultra-IHC employing PBS containing 3% BSA encountered non-specific staining through the unexpected anti-BSA antibody that had contaminated the secondary antibody reagent. Affinity-purified secondary antibody reagent might be free from such contamination. As mentioned in the following chapter of enzymatic-AR and ultra-IHC of Tax, non-specific staining in B-cell malignant lymphoma cells may be that of a part of an antibody known as the Fc (Fragment, crystallizable) region. This kind of non-specific staining cannot be suppressed by the PBS containing 0.25% casein and the nsCSA system may require additional Protein block with PBS containing 8% horse serum prior to the primary antibody reaction and with PBS containing 8% goat serum prior to the secondary antibody-polymer reagent reaction.

Furthermore, an adequate concentration of CARD reaction-amplification reagent must be determined because the amplification reagent of FITC-labeled tyramide from the CSA II system yielded a larger amount of non-specific staining than that of biotinylated tyramide from the nsCSA system [28].

III. Application of Ultra-IHC of HTLV-1 Tax to Etiological Diagnosis of ATLL and Related Lesions

The pathogenicity of HTLV-1 infection that causes ATLL is thought to be that of Tax, where Rex modulates Tax expression and reproduction of HTLV-1 (Fig. 1) [110]. The molecular mechanisms in Tax pathogenicity have been clarified and the target molecules of Tax are summarized in Table 2 according to Grassmann *et al.* [23] and Watanabe [106]. Recently, the pathogenicity of HBZ mRNA and protein was analyzed [64, 65]. In addition, Tax, Rex and HBZ proteins are thought to modulate the activation of HTLV-1-proviral DNA and host genes together. Therefore,

Table 2. *Targets and present form of HTLV-1 Tax*

Target	Effect and present form of Tax	References
HTLV-1		
LTR	Direct effect, forming a Tax-CREB-LTR's CRE-motif complex.	[1, 10, 11, 91, 112]
Host cells		
TBP	Direct effect, forming a Tax-CBP complex or a Tax-p300-CAF complex with TBP.	[12, 14]
Signal transduction in host cells		
NF-κB	Direct binding, forming a Tax-IKKg (=NEMO) complex and a Tax-NF-κB-CBP complex	[15, 26, 41, 46]
IL-2 and IL-2 receptor (IL-2R)	Indirect up-regulation	[3, 7, 9, 22, 38, 66, 68, 81, 85]
IL-15 and IL-15 specific receptor (IL-15R)	Indirect activation	[8, 63]
IL-13	Indirect up-regulation	[16, 103]
OX40 and OX40L	Indirect up-regulation	[78]
Transforming growth factor beta 1 (TGF-β1)	Indirect repression	[6, 54, 56]
Kinase-cascades in host cells		
PI3K and its downstream target Akt	Unclear	[60]
ERK-JNK cascade	Unclear	[48, 107]
Cell cycle dysregulation in host cells		
Cdk4, Cdk6 and Cdk2	Direct effect, forming a Tax-Cdk2/4/6 complex	[24, 25, 43, 58, 72, 73]
Cdk inhibitors ($p16^{INK4A}$, $p15^{INK4B}$, $p18^{INK4c}$, $p19^{INK4d}$ and $p27^{Kip1}$)	Direct repression, forming Tax-$p16^{INK4A}$ and -$p15^{INK4B}$ complexes, and indirect suppression ($p18^{INK4c}$, $p19^{INK4d}$ and $p27^{Kip1}$)	[2, 43, 61, 93, 94]
Cyclin E	Indirect up-regulation	[39, 43, 83]
Cyclin D	Indirect up-regulation	[2, 20, 43, 69, 83]
Rb protein	Direct effect, forming a Tax-Rb protein complex	[52, 73]
E2F	Indirect up-regulation	[57, 75]
Cyclin A	Indirect suppression	[53]
ChK 1 and Chk 2	Indirect interaction	[79]
APC	Direct effect, forming a Tax-APC complex	[59]
Cellular checkpoint protein MAD1	Direct effect, forming a Tax-MAD1 complex	[44, 47]
Tumor suppressors and cellular apoptosis in host cells		
p53 and $p21^{Waf1/Cip1}$	Indirect or direct inactivation, forming a Tax-p300/CBP co-activator complex	[5, 102]
hDLG	Direct effect, forming a Tax-hDLG complex	[37, 95]
DNA repair and maintaining chromosomes in host cells		
DNA polymerase β and BER	Indirect suppression	[45]
DNA polymerase δ, NER and mismatch repair.	Indirect suppression	[49]
BclxL that suppresses RAD51 recombination pathway, suppressing homologous recombination.	Induction	[82]
hTERT	Indirect induction	[21, 90]

LTR: Long terminal repeat of HTLV-1 proviral DNA. CREB: Cyclic-AMP-response element binding protein. CRE: Cyclic-AMP responsive. TATA box: Goldberg-Hogness box. TBP: TATA box-bound protein. CBP: CREB-binding protein. CAF: CBP-associated factor. NF-κB: Nuclear factor kappa B. IKKg: I-kappaB-kinase gamma. IKKg=NEMO: NF-κB essential modulator. OX40=CD134: A member of the tumor necrosis factor (TNF)-receptor family and co-stimulatory T-cell molecule. OX40L: OX40 ligand. PI3K: Phosphoinositide 3-kinase. Akt=Protein kinase B (PKB). ERK: Extracellular signal-regulated kinase. JNK: C-Jun NH_2-terminal kinase. Cdk: Cyclin-dependent kinase. Rb protein: Retinoblastoma protein. ChK: Checkpoint kinase. APC: Anaphase promoting complex. hDLG: Human DLG, a homologue of the Drosophila discs large PDZ domain-containing tumor suppressor. BER: Base excision repair. NER: Nucleotide excision repair. hTERT: Human telomerase reverse transcriptase.

the minimum target-molecules in ultra-IHC for etiological diagnosis of ATLL were Tax and Rex, while the histochemistry of HBZ mRNA and protein is currently expected to be established.

a) Modified ImmunoMax/CSA method for Tax and Rex on formalin-fixed paraffin-embedded sections

The rat monoclonal antibody against Tax, WATM-1 [100], mouse monoclonal antibody against Tax, Lt-4 [55], and mouse monoclonal antibody against Rex, Rec-6 [30] were supplied by Dr. Y. Tanaka (Table 3). Sections of the HTLV-1-related cell line MT-2 were obtained from formalin-fixed and paraffin-embedded cell pellets. ATLL formalin-fixed paraffin-embedded sections were archival pathology specimens of lymph nodes diagnosed as ATLL. The modified ImmunoMax/CSA method was performed by a semi-autostainer (MicroProbe™, Fisher Scientific Co.) [30, 31, 62]. Heating-AR was performed, heating sections in 4 M urea solution by pressure cooking for 5 min [30]. Negative control staining was that of the primary antibody reaction employing antibody dilution solution containing no primary antibody.

By means of the heating-AR and ordinary sensitive polymer method (Fig. 2d), only Lt-4 showed faint staining in MT-2 while the other antibodies revealed no staining in MT-2 and ATLL. By means of the heating-AR and modified ImmunoMax/CSA method, in comparison with the negative control (Fig. 3a), MT-2 indicated strong expression of WATM-1-labeled Tax (Fig. 3b) and weak expression of Rec-6-labeled Rex (Fig. 3c). In comparison with the negative control (Fig. 3d), ATLL exhibited weak expression of WATM-1-labeled Tax (Fig. 3e) and obvious expression of Rec-6-labeled Rex (Fig. 3f).

It was suggested that it is possible to detect Tax and Rex on archival pathology specimen sections by means of heating-AR and ultra-IHC. Moreover, it was indicated that there was a difference in Tax and Rex expression pattern between MT-2 and ATLL.

b) Application to case study of ATLL and related lesions

We identified HTLV-1-associated non-neoplastic lymphadenopathy (HANNLA) in HTLV-1 carriers [33]. HANNLA demonstrated atypical follicular hyperplasia, follicle-lysis, and enlarging paracortex associated with somewhat atypical lymphocytes [33]. Atypical follicles were also noted in the tonsil of HTLV-1 carriers [97]. Gradual increased expression of Lt-4 and WATM-1-labeled Tax and high expression of Rec-6-labeled Rex was detected by the heating-AR and modified ImmunoMax/CSA method in atypical lymphocytes in the enlarged paracortex of HANNLA, where marked expression of Ia-like antigen was observed, and an increased number of HTLV-1 proviral DNA copies were estimated semi-quantitatively from polymerase chain reaction (PCR) for HTLV-1 proviral DNA and a host cell gene [30]. It was suggested that HTLV-1-infected non-neoplastic T-cells expressed Tax and Rex in the proliferative lesion, possibly related to occurrence of anti-HTLV-1 immunity.

A smoldering type ATLL manifested as erythema in the bilateral dorsal aspects of the upper arms, the fore chest, the back, the abdomen, and the bilateral anterior aspects of the thigh, and as hyperkeratotic erythema in the bilateral aspects of the toes in a 76-year-old Japanese man. Biopsied erythema in the left aspect of the thigh showed epidermotropism of lymphocytes with their intraepidermal microabscess formation (Fig. 4a), their perivascular infiltration in the upper dermis (Fig. 4b) and their infiltration to hair follicles (Fig. 4c). A biopsied lymph node in the left inguinal region demonstrated dermatopathic lymphadenopathy (DPLA) with hyperplastic lymph follicles and enlarged paracortex (Fig. 4d) where atypical lymphocytes proliferated (Fig. 4e) and comprised $CD4^+$ (Fig. 4f) $CD8^-$ T-cells. Southern blot analysis of DNA extracted from the left inguinal lymph node indicated monoclonal integration of HTLV-1 proviral DNA (Fig. 4j), shown as 1 band in EcoR1 digestion, 3 HTLV-1 proviral DNA bands, and no detection of 2 virus-cellular junction bands in Pst1 digestion. These lesions were diagnosed as that of smoldering ATLL. The heating-AR and modified ImmunoMax/CSA method showed that some ATLL cells proliferating in the paracortex of the left inguinal lymph node expressed weakly WATM-1-labeled Tax (Fig. 4h) and that many of them expressed Rec-6-labeled Rex (Fig. 4i). It was suggested that proliferating ATLL cells in smoldering type expressed Tax weakly and Rex strongly, identical to that of the ATLL in Figure 3.

ATLL initiating in the right palate tonsil and infiltrating to the cervical and axillary lymph nodes was observed in a 51 year-old Japanese woman. She manifested swelling of the right palate tonsil that showed diffuse proliferation of small to medium-sized cells (Fig. 5a and b) with $CD3^+$ $CD4^+$ T-cell phenotype. One month later, a swollen right palate tonsil and right cervical and axillary lymph nodes (Fig. 5c) revealed infiltrative proliferation of medium-sized to large $CD3^+$ $CD4^+$ $CD30^+$ T-cells (Fig. 5d and e) with developing background meshwork of thymidine phosphorylase $(TP)^+$ dendritic cells (Fig. 5f). DNA extracted from the right axillary lymph node indicated oligoclonal integration of proviral DNA, shown as 2 bands in EcoR1 digestion, 3 proviral DNA bands, and 3 weakly labeled virus-cellular junction bands in Pst1 digestion (Fig. 5j), which differed from those of a defective HTLV-1 provirus [23, 99]. Rearrangement of T-cell receptor β was noted (Fig. 5k). This case was an early phase of ATLL developing from small- to medium-sized cells to pleomorphic cells with a $CD30^+$ activating phenotype. In the heating-AR and modified ImmunoMax/CSA method, most ATLL cells in early phase ATLL in the right axillary lymph node showed obvious expression of WATM-1-labeled Tax (Fig. 5h) and much stronger expression of Rec-6-labeled Rex (Fig. 5i) without obvious staining in the negative control (Fig. 5g), suggesting that early ATLL cells with the activating phenotype expressed Tax in an obvious manner.

ATLL was also observed in Native Americans in Argentina [62]. All 5 Native American ATLL cases demon-

Table 3. *Antibodies that appeared in this review*

Antigen	Antibody	Antigen retrieval	Detection method
Used for diagnosis of lymphomas			
CD3	NCL-CD3-PS1, Novocastra	Heating*	Ordinary-IHC #1
CD4	NCL-CD4-IF6, Novocastra	Heating*	Ordinary-IHC #1
CD8	M7103, Dako	Heating*	Ordinary-IHC #1
CD30 (Ber H2)	M0751, Dako	Heating*	Ordinary-IHC #1
Thymidine phosphorylase (TP)	Supplied from Dr. Akiyama S	Heating*	Ordinary-IHC #1
CD5	Leu 1, Becton Dickinson	Heating**	Ultra-IHC #2
Used for detecting HTLV-1 related proteins			
HTLV-1 p40Tax	Mouse mAb, Lt-4, supplied from Dr. Tanaka Y	Heating*, Enzymatic***	Ultra-IHC #2,3
HTLV-1 p40Tax	Rat mAb, WATM-1, supplied from Dr. Tanaka Y	Heating*, Enzymatic***	Ultra-IHC #2,3
HTLV-1 p27Rex	Mouse mAB, Rec-6, supplied from Dr. Tanaka Y	Heating*	Ultra-IHC #2
Used for detecting proliferation, cell cycle and DNA-damaged cell death			
Ki67 antigen (MB-1)	M7240, Dako	Heating*	Ultra-IHC #3
p53	NCL-p53-DO7, Novocastra	Heating*	Ultra-IHC #3
p53 phosphorylated	NCL-p53-PHOS, Novocastra	Heating*	Ultra-IHC #3
E2F-1	sc193, Santa Cruz	Heating**	Ultra-IHC #2
E2F-4	sc511, Santa Cruz	Heating**	Ultra-IHC #2
DP-1	sc610, Santa Cruz	Heating**	Ultra-IHC #2
Cyclin E	NCL-CYCLIN E, Novocastra	Heating**	Ultra-IHC #2
Used for detecting autophagy (autophagic vesicle nucleation)			
Beclin-1	sc11427, Santa Cruz	Enzymatic***	Ultra-IHC #3
Used for detecting stem cells, fetal cells, cancer cells and lymphoma cells			
Survivin	ab469, Abcam	Heating****	Ordinary-IHC #1
CD117	NCL-CD117, Novocastra	Heating*	Ultra-IHC #3

*: Antigen retrieval heating in 0.01 M citrate buffer pH 6.
**: Antigen retrieval heating in 4 M urea solution by pressure cooking for 5 to 10 min in a draft.
***: Antigen retrieval treating sections by proteinase K solution for 10–30 min at room temperature.
****: Antigen retrieval heating in Diva Decloaker buffer (Biocare Medical) independent from pH of solution.
#1: Ordinary-IHC, super sensitive indirect enzyme-labeled antibody method (enzyme- and secondary antibody-labeled polymer reagent method).
#2: Ultra-IHC (Modified ImmunoMax/CSA method, possibly new simplified CSA system and Dako CSA II system modified according to the new simplified CSA system).
#3: Ultra-IHC (New simplified CSA system).

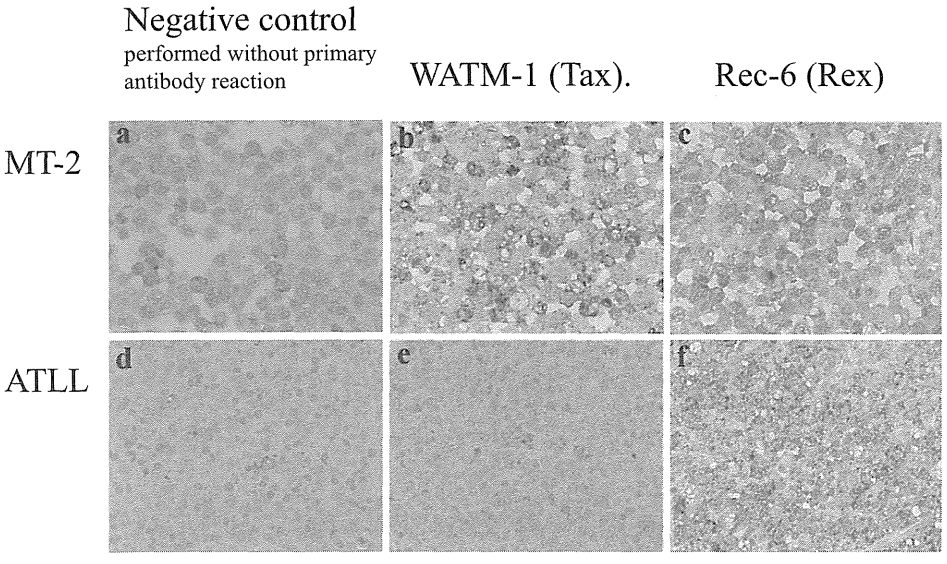

Fig. 3. The modified ImmunoMax/CSA method of Tax and Rex on paraffin sections of MT-2 and 1 case of lymphoma type ATLL (DAB-H_2O_2 reaction with methyl green nuclear counterstaining. ×40, Olympus BX50, FUJIFILM HC-300). **a–c**) MT-2. **d–f**) ATLL. **a** and **d**) Negative control staining performed with antibody dilution fluid containing no primary antibody. **b** and **e**) WATM-1 (Tax). **c** and **f**) Rec-6 (Rex). In comparison with the negative control staining (**a, d**) MT-2 cells show stronger Tax staining (**b**) than ATLL (**e**) does, although ATLL cells show stronger Rex staining (**f**) than MT-2 (**c**) does.

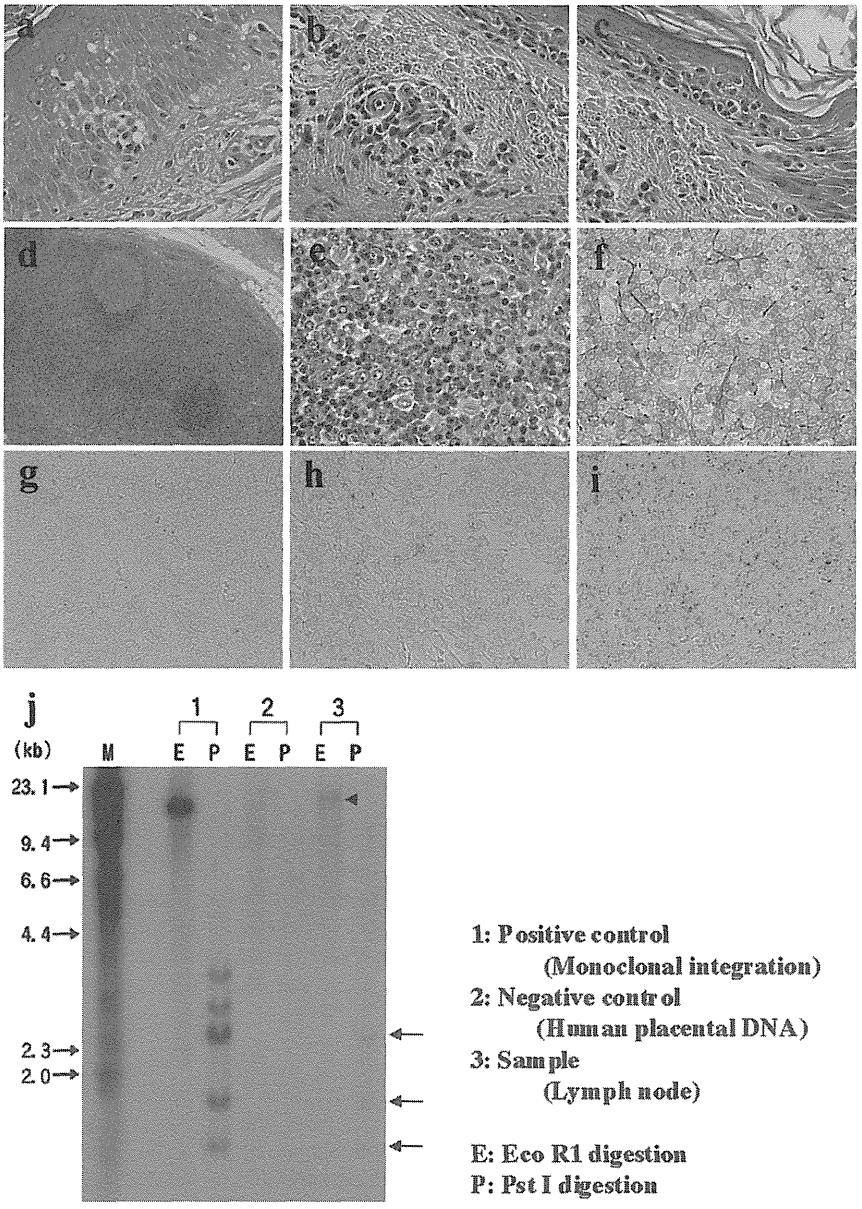

Fig. 4. Tax and Rex Expression in smoldering type ATLL (×40, Olympus BX50, FUJIFILM HC-300). **a–e**) Haematoxylin & Eosin (H.E.). **a–c**) The left thigh showed intra-epidermal microabscess formation (**a**) and infiltration of small atypical lymphocytes around capillaries in the upper dermis (**b**) and into the hair follicle (**c**). **d–i**) The left inguinal lymph node. **d**) Low power view (×10). **e**) High power view of the enlarged paracortex. **f**) Ordinary-IHC of CD4 (DAB-H_2O_2 reaction and haematoxylin nuclear counterstaining). The left inguinal lymph node demonstrates dermatopathic lymphadenopathy, of which the enlarged paracortex (**d**) indicates proliferation of atypical lymphocytes (**e**) positive for CD4 (**f**). **g–i**) The modified ImmunoMax/CSA method (DAB-H_2O_2 reaction with methyl green nuclear counterstaining) for negative control performed without primary antibody (**g**), WATM-1 for Tax (**h**), and Rec-6 for Rex (**i**). In comparison with the negative control staining (**g**) some cells express Tax (WATM-1) weakly (**h**) and many cells express Rex (Rec-6) strongly (**i**). **j**) Southern-blot analysis of HTLV-1 proviral DNA integration. 1) Positive control (ATLL cell line), 2) Negative control (human placental DNA), and 3) DNA extracted from the left inguinal lymph node. E) EcoR1 digestion. Two DNA sequence (GAATTC) in cellular DNA on both ends of the HTLV-1 proviral DNA are digested. P) Pst1 digestion. The DNA sequence (CTGCAG) in HTLV-1 proviral DNA and in cellular DNA on both ends of the HTLV-1 proviral DNA is digested into 3 proviral DNA bands of 1.2 kb, 1.8 kb, 2.5 kb and 2 virus-cellular junction bands. Positive control (1: Monoclonal integration of HTLV-1 proviral DNA in ATLL cell line) shows 1 band labeled by a whole HTLV-1 proviral DNA probe in EcoR1 digestion and 3 proviral DNA bands and 2 virus-cellular junction bands in Pst1 digestion. The DNA extracted from the left inguinal lymph node (3) indicates 1 weak band in EcoR1 digestion (arrow-head) and 3 weak bands of 1.2 kb, 1.8 kb, 2.5 kb in Pst1 digestion (arrows) while 2 virus-cellular junction bands are not recognized, suggesting monoclonal integration of HTLV-1 proviral DNA in some atypical cells.

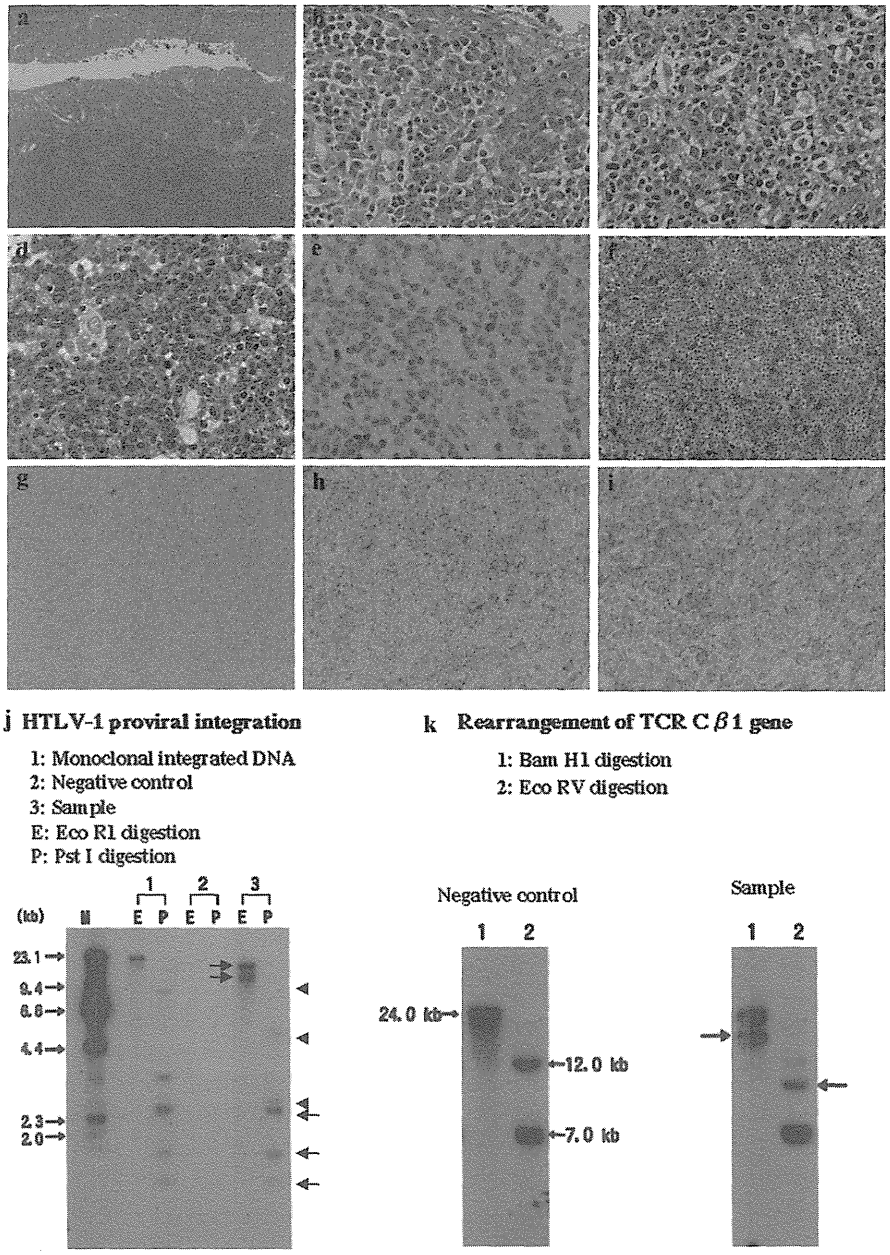

Fig. 5. Tax and Rex expression in ATLL that initiated in the right palate tonsil and infiltrated to the cervical and axillary lymph nodes (×10 or ×40, Olympus BX50, FUJIFILM HC-300). **a** and **b**) First biopsy of the right palate tonsil (H.E.) showing diffuse proliferation of medium-sized ATLL cells (**a**, ×10) and their tropism to the tonsillar epithelia (**b**). **c–i**) Second biopsy of the right axillary lymph node. **c**) Diffuse proliferation of pleomorphic ATLL cells can be observed (H.E.). **d–f**) Ordinary-IHC of CD4 (**d**), CD30 (**e**) and thymidine phosphorylase (TP, **f**) (DAB-H_2O_2 reaction and haematoxylin nuclear counterstaining). Most of the pleomorphic ATLL cells are CD4 T-cells (**d**), some of them express CD30 (**e**), and associate symbiotic growth of TP-positive dendritic cells forming a meshwork. **g–i**) The modified ImmunoMax/CSA method for the negative control (**g**), WATM-1 for Tax (**h**), and Rec-6 for Rex (**i**) (DAB-H_2O_2 reaction and haematoxylin nuclear counterstaining). In comparison with the negative control staining (**g**), expression of Tax (WATM-1) (**h**) and strong expression of Rex (Rec-6) (**i**) are detected in the pleomorphic ATLL cells. **j**) Southern-blot analysis of HTLV-1 proviral DNA integration. 1) Positive control (ATLL cell line), 2) Negative control (human placental DNA), and 3) Sample: DNA extracted from the left axillary lymph node. E) EcoR1 digestion. P) Pst1 digestion. The extracted DNA shows 2 DNA bands from EcoR1 digestion, and 3 proviral DNA bands (arrows) and 3 virus-cellular junction bands (arrow heads) from Pst1 digestion, suggesting oligoclonal integration of proviral DNA in the ATLL cells. **k**) Southern-blot analysis of T-cell receptor β (TCR β). 1) BamH1 digestion. BamH1 digests the DNA sequence (GGATCC) in cellular DNA on both sides of the TCR β DNA sequence. 2) EcoRV digestion. EcoRV digests the DNA sequence (GAATTC) in the TCR β DNA sequence. A rearranged TCR β band is observed in BamH1 (arrow) and EcoRV digestion (arrow) of the sample, suggesting that these pleomorphic ATLL cells are monoclonal αβ T-cells.

Table 4. *Evaluation of E2F, DP-1 and cyclin E in MT-2, ATLL and peripheral T-cell lymphomas in Europeans (EPTL), detected by the heating-AR and modified ImmunoMax/CSA method*

	HTLV-1			E2F		DP-1	Cyclin E
	Proviral DNA	Tax	Rex	E2F-1	E2F-4		
MT-2	integrated	+++	++	–	++	+++	–
ATLL 1	integrated	+	+++	–	+++	+++	++
ATLL 2	integrated	+	+++	–	–	+++	++
ATLL 3	integrated	+	++	–	–	++	++
ATLL 4	integrated	+	++	–	–	++	++
ATLL 5	integrated	+/–	++++	+	–	++	+
ATLL 6	integrated	+/–	++	–	–	+/–	–
ATLL 7	integrated	+/–	++	–	–	++	+
ATLL 8	integrated	–	+++	+++	–	+++	+
ATLL 9	integrated	–	+++	–	++	–	+
EPTL 1	n.e.	n.e.	n.e.	+++	+++	++	++
EPTL 2	n.e.	n.e.	n.e.	++	+/–	+++	+++
EPTL 3	n.e.	n.e.	n.e.	++	+	+++	+++
EPTL 4	n.e.	n.e.	n.e.	+	+/–	++	+++
EPTL 5	n.e.	n.e.	n.e.	+	–	+++	++
EPTL 6	n.e.	n.e.	n.e.	+/–	+/–	+++	+++
EPTL 7	n.e.	n.e.	n.e.	–	+/–	+++	+++
EPTL 8	n.e.	n.e.	n.e.	+/–	–	+++	++
EPTL 9	n.e.	n.e.	n.e.	–	–	+++	+

ATLL: Adult T-cell leukemia, lymphoma type. EPTL: Peripheral T-cell lymphoma in European, diagnosed in Dept. of Pathology (Prof. Martin-Leo Hansmann), Johann Wolfgang Goethe-Universität Frankfurt am Main.
[HTLV-1 proviral DNA] Integrated: HTLV-1 proviral DNA was shown to be integrated in lymphoma cells. n.e.: Not examined.
Evaluation of the immunostainig of the modified ImmunoMax/CSA method of Tax, Rex, E2F-1, E2F-4, DP-1, and Cyclin E. –: Not positive cells. +/–: Rare very weakly positive cells. +: A few weakly positive cells. ++: Some moderately positive cells. +++: Many strongly positive cells. ++++: Almost all very strongly positive cells. n.e.: Not examined.
ATLL Tax vs. Cyclin E: Wilcoxon signed-ranks test, p=0.0209.

strated obvious Tax and strong Rex expression, respectively, in archival sections of pathology specimens tested by the heating-AR and modified ImmunoMax/CSA method using WATM-1 and Rec-6 [62]. However, 2 of 9 Kagoshima ATLL cases did not demonstrate positive staining of WATM-1-labeled Tax with the heating-AR and modified ImmunoMax/CSA method (Table 4).

Clinically, approximately half of all ATLL cases are leukemia, and the patients' lymph nodes were usually not examined pathologically. A lump of naturally precipitated and coagulated peripheral blood can be processed into a formalin-fixed and paraffin-embedded specimen, i.e., peripheral blood tissue specimen (PBTS) [35]. Leukemic ATLL cells in the PBTS can be examined in the same manner as those in archival pathology specimens. In PBTS of 6 of 8 leukemic type ATLL cases comprising 4 chronic and 4 acute leukemia type cases, Tax and Rex were detected weakly and strongly, respectively, in a few or some ATLL cells with the heating-AR and modified ImmunoMax/CSA method using WATM-1 and Rec-6 [35].

HTLV-1-infected T-cells in the proliferative lesion in the paracortex of HANNLA and ATLL cells proliferating in the paracortex of DPLA in smoldering ATLL and in the lymph nodes in early phase lymphoma type ATLL and in lymphoma type ATLL in Native Americans and in Japanese (Kagoshima natives) expressed Tax weakly and Rex strongly with the heating-AR and modified ImmunoMax/CSA method. Tax expression was correlated to Ki67 antigen$^+$ proliferating cells in PBTS of leukemia type ATLL [35]. A present form of Tax retrieved by heating AR and detected with the modified ImmunoMax/CSA method of WATM-1 against Tax may be related with ATLL cell proliferation.

c) Enzymatic-AR and ultra-IHC of Tax

Tax is synthesized from the integrated HTLV-1 proviral DNA pX region. As listed in Table 2, Tax forms a complex with cyclic-AMP-response element binding protein (CREB), docks at cyclic-AMP responsive (CRE)-motifs of the HTLV-1 proviral DNA long terminal repeat (LTR) and up-regulates Tax synthesis [1, 10, 11, 42, 91, 112]. On the other hand, Tax binds directly TATA box-bound protein (TBP), recruits CREB-binding protein (CBP), p300 and p300/CBP-associated factor (P/CAF) and forms Tax-CBP-p300 and Tax-P/CAF complexes [12, 14], trans-activating or -suppressing host cells genes. Besides, Tax binds directly I-kappaB-kinase gamma (IKKg, =NEMO: NF-κB essential modulator) and indirectly up-regulation of Nuclear factor kappa B (NF-κB), effecting down-stream